Remote sensing of freshwater habitats for large rivers and lakes of the Waikato region using sub-pixel classification

CBER Contract Report 63

A report prepared for
Environment Waikato

by

Salman Ashraf[1], Lars Brabyn[2], Brendan J. Hicks[1]

salman@waikato.ac.nz, b.hicks@waikato.ac.nz, larsb@waikato.ac.nz

[1]Centre for Biodiversity and Ecology Research
Department of Biological Sciences

[2]Department of Geography, Tourism and Environmental Planning

The University of Waikato
Private Bag 3105
Hamilton, New Zealand

14 September 2007

THE UNIVERSITY OF WAIKATO
Te Whare Wānanga o Waikato

CBER University of Waikato
Centre for Biodiversity and Ecology Research

Table of Contents:

List of Figures:

List of Tables:

List of Abbreviations:

ADAR	Airborne Data Acquisition and Registration
AGDS	Acoustic Ground Discrimination System
ALOS	Advance Land Observing Satellite
ASTER	Advance Spaceborne Thermal Emission and Reflection Radiometer
ATM	Airborne Thematic Mapper or Airborne Topographic Mapper
CDOM	Coloured (*or Chromophoric*) Dissolved Organic Matter
ETM+	Enhanced Thematic Mapper Plus
HRG	High Resolution Geographic
HRV	High Resolution Visible
HRVIR	High Resolution Visible Infra Red
LIDAR	Light Detection and Ranging
LISS	Linear Imaging Self-scanning Sensor
RADAR	**Ra**dio **D**etection **a**nd **R**anging
SSC	Suspended Sediment Concentration
SONAR	**So**und **N**avigation **a**nd **R**anging
SPOT	**S**atellite **P**our l'**O**bservation de la **T**erre
TM	Thematic Mapper

Reviewed by: *Approved for release by*:

Kevin J. Collier David P. Hamilton

Executive Summary:

The overall goal of this study was to evaluate the feasibility of multi-sensor and multi-spectral remote sensing data for mapping different freshwater habitat zones of large rivers and lakes of the Waikato region. This has been achieved by addressing the following objectives:

1. Reviewing relevant literature on different remote sensing techniques to map vegetation in littoral zones, riparian buffers, and floodplains. This also includes literature on monitoring water parameters using remote sensing.
2. Identifying different sources of high to medium spatial resolution remote sensing data suitable for this research, and assessing its availability for the Waikato region. This includes an archival search and the request for new acquisitions, if necessary.
3. Trialling assessments of remote sensing capabilities using broad image processing techniques on existing and archived satellite and aerial photographic data, and;
4. Making recommendations to develop remote sensing capabilities to regularly monitor the specified ecological conditions of large rivers and lakes.

The review of satellite sensors available in NZ for aquatic mapping has identified three data options, which have been purchased for a case study area (Tongariro river delta). These data options are Landsat-5 (30m resolution), ALOS (10m and 2.5m), and QuickBird-2 (2.4m and 0.6m). There is no one perfect option available as each option is a compromise between spatial and spectral resolution, and cost. The Quickbird-2 option may be feasible if the "Kiwimage" initiative to purchase Quickbird-2 data for all of NZ eventuates. Developing tools and classification techniques using Quickbird-2 could potentially be very useful to Environment Waikato for mapping aquatic environments if "Kiwimage" eventuates. ALOS also provides a cost effective option, especially if the non-commercial pricing available to the Waikato University is used. The main problem with ALOS, being a recent satellite, is the limited archive of images for Waikato, as this is a recent satellite. The availability for the Waikato region, which is often cloudy, may cause problems. Landsat-5 offers an extensive archive and relatively cheap acquisition with good spectral resolution but compromised spatial resolution. The combination of Landsat 5 and ALOS may produce a feasible option for regular mapping of aquatic environments. In addition to satellite images there is also existing WRAPS aerial images with 1m spatial resolution. These images could possibly be used in combination with satellite images.

It is recommended to compare different classification algorithms such as supervised and sub pixel classification using the ALOS, Landsat-5, Quickbird-2, and WRAPS images. To obtain the most from these data sets, it is also recommended to collect *in-situ* spectral reflectance data for predominant species and species assemblages (of terrestrial, emergent and submerged vegetation) at different water quality parameters for the case study area. This will improve sub pixel classification accuracy. An alternative or complimentary approach could be to investigate the use of a digital camera for taking vertical aerial images.

Chapter 1

Introduction

Environment Waikato wishes to explore the feasibility of mapping the ecological condition along the margins of the large water bodies (lakes and large rivers) using remote sensing. This is because conventional field based mapping based on direct ground surveys are labour intensive and feasible only for small and easily accessible areas (Nelson et al., 2006). Also riparian vegetation is heterogeneous and features tend to be very small and irregular. Capturing this type of detail with conventional manual mapping is not cost effective (Congalton et al., 2002). Information on lake and large river systems within the Waikato Region is limited and mostly focused on particular areas such as the Waikato River, Lake Taupo and the Waipa Peat Lakes. River water quality has been routinely monitored in the Waikato region since 1980. Since 1993, water quality is now systematically measured at ten sites on the Waikato River and over 100 sites on important lakes and other rivers and streams, with results being reported annually (Barnes, 2002; Vant and Smith, 2004). Similarly, to assess lake ecological conditions, LakeSPI (Lake Submerged Plant Indicator) is determined for 41 varied-size lakes of the region. This tool ranks different lakes based on its native and invasive submerged plant conditions and provides an overall ecological condition of the lake (Edwards et al., 2007).

Remote sensing offers a potential tool for mapping and monitoring the physicochemical characteristics and ecological condition of areas inundated by freshwater, such as littoral, riparian and floodplain zones. The habitat characteristics that can be obtained from remotely sensed information may include landcover types, the identification of vegetation species and information on water parameters such as turbidity, chlorophyll-*a* concentration, water temperature and depth index.

The current research looks into mapping and monitoring three distinct but contiguous habitat zones associated with the freshwater. These are:

i) Inland riparian buffers,
ii) Emergent and shallow submerged aquatic vegetation along rivers or around wetlands, and
iii) Water quality of the water bodies.

Each of these habitat zones requires separate data and image processing techniques to map and regularly monitor. It has been learnt from previous studies (Shanmugam et al., 2006; Valta-Hulkkonen et al., 2003; Vis et al., 2003) that the following four parameters influence the ability to accurately map aquatic vegetation:

- Characteristics of the target habitat which include amount or geometry of foliage, density or openness of the canopies and its phenology.
- Environmental and physical conditions of the surrounding matter (i.e. water and atmosphere) such as water quality (which depends on the concentration of chlorophyll *a* and suspended sediments), height of water column above

vegetation and atmospheric condition, e.g. high concentration of the suspended aerosols such as water or dust due to humidity or other factors.

- Remotely sensed data characteristics and quality.
- Metrological conditions of image capture such as weather and time of day.

1.1. Objective of the study

The overall goal of this study was to evaluate the feasibility of multi-sensor and multi-spectral remote sensing data for mapping different freshwater habitat zones of large rivers and lakes of the Waikato region. This has been achieved by addressing the following objectives:

1. Reviewing relevant literature on different remote sensing techniques to map vegetation in littoral zones, riparian buffers, and floodplains. This also includes literature on monitoring water parameters using remote sensing.
2. Identifying different sources of high to medium spatial resolution remote sensing data suitable for this research, and assessing its availability for the Waikato region. This includes an archival search and the request for new acquisitions, if necessary.
3. Trialling assessments of remote sensing capabilities using broad image processing techniques on existing and archived satellite and aerial photographic data, and;
4. Making recommendations to develop remote sensing capabilities to regularly monitor the specified ecological conditions of large rivers and lakes.

1.2. Fundamentals of remote sensing images

In order to appreciate the choices and characteristics of image acquisition it is necessary to understand the fundamental parameters that need to be considered. The following sections provide important principles that are fundamental to the discussion in this report:

Spatial resolution

Spatial resolution is the size of the pixels that are captured by the sensors. This determines the ability of a sensor to detect an object, which is relative to the size of the actual object. For example, to detect a 25m wide stream, a pixel of similar or smaller size is required, such as a Landsat TM image. To identify its width accurately, a higher spatial resolution is required, such as a SPOT panchromatic data with 10m spatial resolution. In order to analyse the morphology, an even higher resolution data is required, such as IKONOS or Quick Bird images with 1m or better spatial resolution.

Spatial extent (swathe)

Spatial extent is the area covered by one image. This is usually related to the spatial resolution. Satellite images that have high spatial resolution will usually cover a small area. The spatial extent of an image will determine how many images are required to study a particular area. The number of images affects the cost of the study.

Spectral resolution

The spectral resolution refers to the number and widths of the electromagnetic radiation bands that are captured by the sensor. For example a sensor may capture three bands that are in the red, green, and blue spectrum. Every object reflects electromagnetic radiation. This radiation can span the fully spectrum from blue light, which has a small wave length to far infra-red which is non visible to the human eye and has a relatively large wave length. An object will have a particular electromagnetic radiation response which is referred to as the radiometric signature. For example green vegetation has a high reflectance of the green wave length. A sensor records such information in bands of different wavelengths. Sensors also vary in the number of bands that are recorded. Given the complexity of aquatic vegetation communities, the spectral resolution is an important parameter in remote sensing. Remote sensing sensors vary in spectral resolution from very broad spectral bands (panchromatic), to multiple discrete bands (multispectral) or to contiguous and very narrow bands (hyperspectral).

Radiometric resolution

Radiometric resolution refers to how precisely a sensor can measure a particular wavelength band. For example a sensor could distinguish 16 classes of green or it could measure 32 classes of green depending on its radiometric resolution. The radiometric resolution of an imaging system describes its ability to discriminate very slight differences in electromagnetic radiation. The finer the radiometric resolution of a sensor the more sensitive it is to detecting small differences in reflected or emitted energy. It is measured in levels of gray scale within an image. Conventional RS data is captured in 256 (equivalent to 2^8 or 8bit) gray intensity levels. Computer graphics inherently work with 24bit colour display which is achieved with the additive mixing of 8bit data captured in three different spectral bands. Some satellites offer greater radiometric resolution than 8bit (up to 12bit or 4096 gray levels). This data is not possible to display on computer screens with enhanced contrast; however, its higher radiometric resolution contributes mathematically to identify subtle variations in the reflectance of different features and thus improves classification results.

Temporal resolution

Temporal resolution refers to the frequency of image acquisition for a given area. It is the revisit period of a satellite to pass over the same area and refers to the length of time it takes for a satellite to complete one entire orbit cycle. A concept of temporal resolution is important when regular monitoring is required. The revisit period of a satellite sensor is usually several days which depends upon its spatial coverage (or swathe). For wide swathe satellites, the repeat period is less than the narrow swathe satellites. Landsat satellites with 185km swathe require 16 days to revisit the same area on the equator. Spot satellites, however, capture images with narrow swathes (60km) and need 26 days to revisit the same area. To overcome this limitation, narrow swathe satellites are usually able to point their sensors to capture off-nadir (side viewing) images while passing over other areas. It also depends on the latitude of the study area.

As remote sensing satellites normally operate in near polar orbits, there is some degree of overlap for the regions close to the poles. As a result, some areas of the Earth tend to be re-imaged more frequently. Thus, the actual temporal resolution of a sensor depends on a variety of factors, including the satellite/sensor capabilities, the swathe width, and latitude. Temporal resolution is important when an area is often cloudy, such as the Waikato, as several passes may be required before a good image is obtained.

Image capture and image processing

Remote sensing is a two stage process. Firstly images need to be captured using aerial photography, or satellite images. An equally important stage is the processing of the image to obtain the information that is required, such as a map of aquatic vegetation zones. There is a wide range of image processing techniques. These techniques are discussed later in this report. Many of these techniques require the use of surveyed field data to "train" the process and validate the process. Some field work is therefore required with image processing.

In recent years, there have been advancements of spatial, spectral and radiometric resolutions of remotely sensed images, both from satellites and digital cameras and scanning systems on airborne platforms as well as enhanced image processing techniques such as sub-pixel classification. These advancements can be used to extract additional information from moderate resolution images thus providing useful information for the management of aquatic ecosystem health, water resources and more detailed characterisation of the narrow littoral and riparian vegetation zone (Goetz, 2006; Shanmugam et al., 2006).

Given the range of remote sensing sensors (from high spatial resolution to hyper-spectral) and techniques currently available (like soft and sub-pixel classifications), the prime interest of this research is to evaluate remote sensing as a cost and time effective tool to map aquatic environments. It is also important to determine the optimum spatial and spectral resolution of remotely sensed data, accuracy, and repeatability of measurements at different scales that are achievable by the different processing techniques.

The second chapter provides a literature review of freshwater aquatic environments and identifies the complexities of mapping this environment using remote sensing. The third chapter focuses on the issues for image capture for the Waikato region and identifies the best choice of images available for mapping freshwater environments. The final chapter makes recommendations for future work.

In addition to this, two appendices provide detailed review of remote sensing platforms and digital sensors and include a historical review of how remote sensing has evolved from aerial photography and photogrammetry. This has been included so that Environment Waikato can contrast photogrammetry, which is presently being used, with satellite and digital imagery.

Chapter 2

Aquatic Remote Sensing

Water constitutes approximately 71% of the earth out of which around 99% is open sea while the remaining percentage is made up from different freshwater habitats including permanent snow cover and glaciers. Despite this small percentage, the surface area under coastal zone and freshwater margins is remarkably high due to its sinuosity i.e. the curving in shape of water and land interaction zones. In addition to high surface area, these regions are highly diverse in terms of flora and geology.

2.1. Types of aquatic habitats

Freshwater habitats can be classified as *fluvial* or *lotic* (running water). This includes rivers or streams or *lentic* (standing water); which is further divided into *lacustrine* (i.e. lakes) or *palustrine* (i.e. marshes). The margins of these freshwater habitats represent a comparatively small but highly diverse, relatively inaccessible continuum of varied size zones, extending from terrestrial regions to deep water. Moving from land towards water, these zones are called riparian and aquatic. The aquatic zone is further divided in the littoral and the limnetic zones.

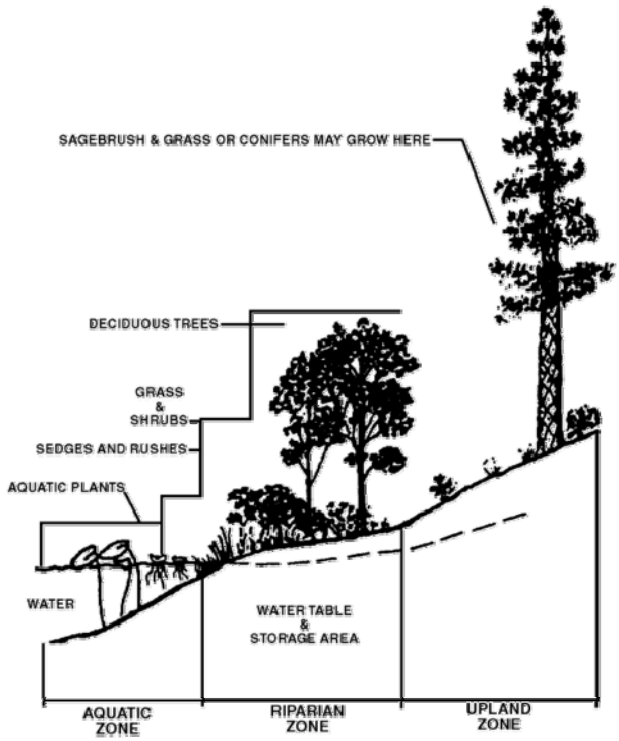

Figure 1: Riparian zone schematic typical of the Florida Everglades.
(Adapted from OEPC, 1994)

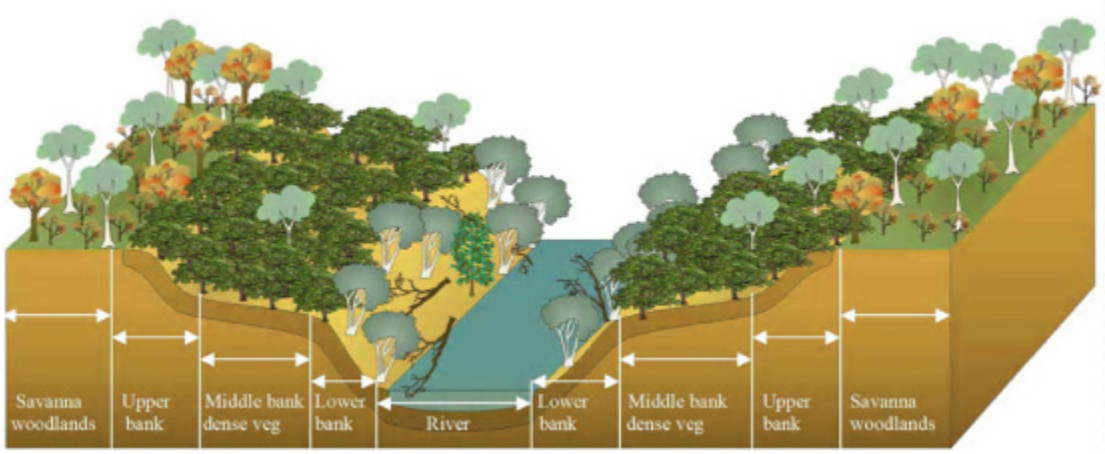

Figure 2: Sketch of the different stream bank sections (riparian zones) identified along the Daly River. (Adapted from Johansen et al., 2007)

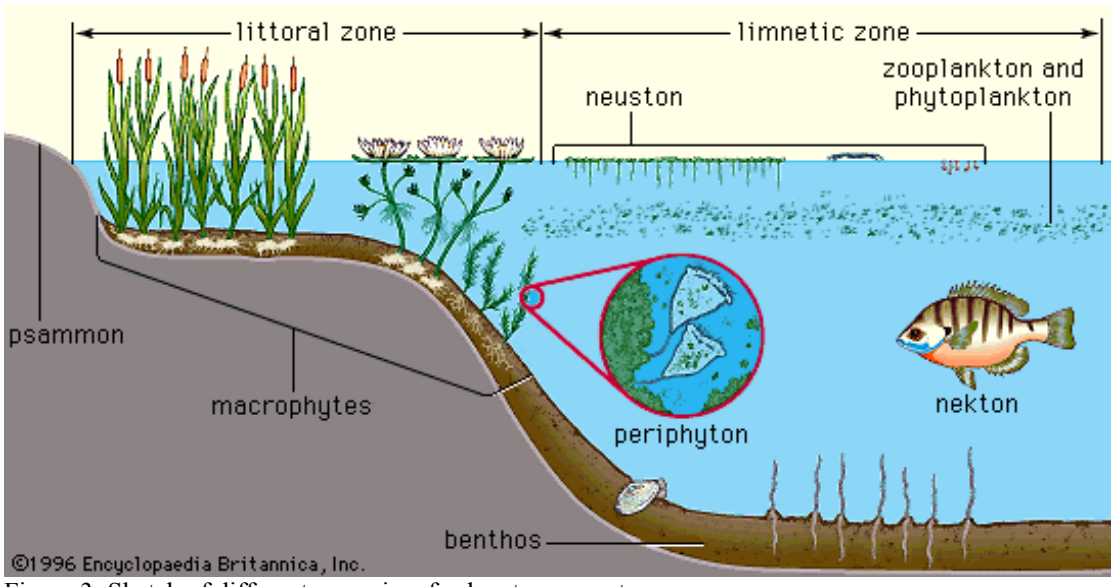

Figure 3: Sketch of different zones in a freshwater ecosystem.
(source: Freshwater: biological communities of lakes. Online Art. Encyclopaedia Britannica Online. 30 May 2007 at URL http://www.britannica.com/eb/art-38)

Aquatic regions are logistically difficult to access which makes them difficult to map using field surveys from land by boat. Such assessments are usually subjective, time consuming and labour intensive and are based on a discrete number of points along transects for each habitat unit (Gilvear et al., 2007). On the other hand, remotely sensed information can be particularly useful for water related habitat assessment because the size of such systems is more conducive to broad spatial analyses (Flotemersch et al., 2006).

Substantial progress has been made in coastal environments where the utility of remote sensing to benthic habitat mapping, such as shallow waters overlying coral reefs and seagrass ecosystems, is more pronounced than in fluvial systems (Bierwirth et al., 1993; Joyce, 2004; Kutser et al., 2006b; Mount, 2006; Sotheran et al., 1997). This research progress in coastal systems highlights the fact that although remotely sensed data can be used to retrieve water depth and substrate characteristics in aquatic environments, the research community needs to undertake 'catch-up' research in relation to fluvial environments (Gilvear et al., 2007).

Different techniques are used for mapping the three freshwater zones because of differences in the amount of water and the type of vegetation found. Therefore, the following sections review these zones separately.

2.2. Remote sensing of riparian buffers

The word "riparian" is derived from the Latin *Ripa*, meaning "river bank". A riparian zone is the interface between land and a flowing surface water body. Riparian zones occur in many forms including grassland, woodland, wetland or even non-vegetative. In some regions the terms riparian woodland, riparian forest, riparian buffer zone or riparian strip are used to characterize a riparian zone. Riparian zones along larger streams and rivers consist of two distinct parallel bands separated by the channel itself. In small, well-vegetated streams a functionally continuous canopy usually exists over the channel (Collier et al., 1995).

Riparian vegetation including floodplain forests along rivers is recognized as an important part of river ecosystems (Muller, 1997). It is an important biodiversity habitat that provides significant biophysical functions. These functions include stream bank stability, filtering of overland flow, shading for temperature and nuisance aquatic plant control, woody debris inputs, cover and spawning habitats for fish species, de-nitrification and nutrient uptake from shallow groundwater (Collier et al., 1995; Goetz, 2006). Riparian vegetation can also convert some forms of toxic chemicals such as pesticides into non-toxic forms through microbial decomposition, oxidation, hydrolysis, and other biodegrading processes occurring in the soil and water (Narumalani et al., 1997).

Remote sensing has been used to a limited extent to map and monitor characteristics of riparian zones with the main focus being on classifying dominant vegetation species and mapping vegetation structural parameters. Due to the limited width of riparian zones and their heterogeneous nature, high spatial resolution image data (≤5 m pixels) are required for mapping most of the riparian zone features related to riparian zone condition and function (Congalton et al., 2002; Goetz, 2006; Johansen and Phinn, 2006a; Johansen and Phinn, 2006b; Johansen et al., 2007). Moreover, Goetz (2006) and Congalton (2006) suggest that these zones should be sampled separately from the upland areas to increase classification accuracy.

Common image analysis techniques used in riparian vegetation studies include digital image classification (i.e. unsupervised and supervised classification), vegetation index clustering, tasselled cap transformation, and image masking mainly using Landsat, SPOT and IKONOS which yielded degraded classification results for low spatial resolution satellites compared to hi-res IKONOS (Apan et al., 2002; Johansen and Phinn, 2006b; Nagler et al., 2001; Narumalani et al., 1997; Weber and Dunno, 2001). Goetz et al. (2003) suggested the timing of data acquisition (thus phenological stage of the riparian habitat), viewing angle and atmospheric conditions as a few limiting factors that can impact the classification accuracy.

Yang (2007) used standard colour aerial ortho-rectified images at 1-2m spatial resolution to map the riparian zone along the Peterson River and Allyn River of the Hunter region in NSW, Australia, and compared classification accuracies with Landsat ETM+ and SPOT-4 data. He concluded that the overall vegetation

classification accuracy for the pilot study area was 81% for digital aerial photography, 63% for SPOT-4, and 53% for Landsat-7 ETM+ using density slicing (parallelepiped) and vegetation indices clustering methods. The main reasons for choosing these methods are that they are relatively simple, widely used in vegetation classification, and applicable to digital aerial photographs.

The accuracy of land or vegetation characterisation from remote sensing data is a function of spatial resolution (Booth et al., 2007; Congalton et al., 2002; Davis et al., 2002; Muller, 1997). Thus moderate resolution data are restricted to coarse descriptive level mapping only (Malthus and Mumby, 2003). In order to determine minimum spatial resolution required to distinguish different riparian vegetation types, Nagler et al. (2005) report that willows could not be distinguished from cottonwoods at 50cm GSD (1:6000). Davis et al. (2002) recommend ≤ 20cm GSD imagery (1:2400) for riparian vegetation monitoring. Lonard et al. (2000) recommend a scale of 1:600 (5cm GSD) to discern woody vegetation types. Booth et al. (2007) describes the collection and utilization of very large scale aerial (VLSA) imagery (~2cm GSD imagery) to illustrate the utility of the data for ecological assessment including comparison of riparian *Proper Functioning Condition* (PFC) assessments made from imagery and on the ground. Riparian PFC is the standard method for assessing how well the physical processes of riparian systems are working and has provided a cost comparison of ground and aerial methods which clearly shows the cost effectiveness of the latter method.

All of the above examples used standard image classification procedures which typically deal with the mixed pixel problem, no matter how refined the spatial resolution of the investigated RS data. This is because traditional per-pixel classification logic has no mechanism for extracting information about the proportion of individual materials of interest within a pixel. A conventional supervised per-pixel or hard classifier assigns each pixel a particular class considering its similarities based on the representative spectral values of the sample data generally referred to as training fields (Lillesand et al., 2004; Verbyla, 1995) thus traditional classifiers generally perform well for classifying large, mono-specific stands of tree species, but they have not been successful in the identification of the proportions of several materials of interest found within the IFOV of a sensor system. However, individual plant species and surface materials that occur as subpixel components in mixed pixels have the potential to be spectrally resolved and classified using subpixel processing techniques that can distinguish surface materials smaller than the spatial resolution of the sensor (Huguenin et al., 1997).

It is assumed that this technique if applied with high resolution RS data may yield better results over per-pixel classification to discern different vegetation types provided that data is captured in a traditional multispectral way i.e. visible to near infra-red band of the electro-magnetic spectrum.

2.3. Remote sensing of littoral zone

Littoral refers to the coast of an ocean or sea, or to the banks of a river, lake or estuary. The word is derived from the Latin *Littor*, which means “shore”. The marine littoral zone is defined as the area between the high water and low water marks. In

freshwater lakes, where tides are usually negligibly small, other definitions of "littoral" must be used.

The littoral zone is one of the most productive ecosystems on Earth, with a gross productivity contributing 19% of the productivity of the entire ocean, with only 6% of its surface area (Gattuso et al., 1998). In the freshwater regime, this zone is home to most of the aquatic plant life both rooted and floating. These macroscopic plants (also called macrophytes) constitute a diverse assemblage of taxonomic groups and are often separated into four categories based on their habit of growth. These are:

1) Emergent macrophytes which are rooted in the substrate but with leaves and flowers extending into the air,
2) Floating-leaved macrophytes which are rooted in the substrate but with floating leaves on the surface of water,
3) Submersed macrophytes which are rooted in the substrate and floating beneath the surface, and
4) Free-floating macrophytes which are not rooted in the substrate and floating on the surface (Brown, 1987; Herbert and Sagarin, 2007).

These various forms of macrophytes generally occur with emergent vegetation nearest the shoreline, then floating-leaved macrophytes, followed by submersed vegetation. Free-floating macrophytes can occur anywhere on the system's surface (Brönmark and Hansson, 2005).

The maximum depth of water to which macrophytes are able to grow (Z_c) in selected North Island lakes show that depth varies significantly for the Waikato region lakes e.g. the depth limit is 5.0m for Rotoroa (Hamilton) lake, 6.0m for Karapiro reservoir and 11.0m for Ohakuri lake (Vant et al., 1986). In later surveys, these limits are further refined as 5.5m and 13.0m for Rotoroa and Ohakuri lakes and 13.0m for Lake Taupo (Schwarz et al., 2000).

Typically, remote sensing has been used to measure macrophytes cover by the labour-intensive visual interpretation process from aerial photographs. In the field of freshwater aquatic botany, a first attempt was made to map aquatic vegetation in Finnish lakes from classification of Landsat satellite image (Raitala et al., 1985). Since then, classification techniques have very much improved, as exemplified by the method of digital image analysis (supervised classification) of aerial photographs proposed by Marshall and Lee (1994) for Canadian lakes to map floating-leafed and emergent forms of these macrophytes. Unfortunately, the supervised classification approach has limited applicability for assessing macrophytes distribution in large regions with many water bodies due to limited spatial coverage per aerial photograph. The spectral signatures required to classify different features in an aerial photograph are not transportable over time and space (Marshall and Lee, 1994).

Therefore, remotely sensed data with large aerial extent are needed to accommodate many lakes in one image for regional monitoring of macrophytes. One approach is to use large swathe satellite images like Landsat Thematic Mapper that include many water bodies within a single image. Although there are other satellite based sensors with a reasonably wide swathe available, they lack the ability to look into the blue part of visible spectrum (e.g. SPOT HRV, HRVIR or HRG and Terra ASTER

sensors) or possess low radiometric resolution (e.g. ResourceSat LISS-III and LISS-IV sensors) to differentiate low reflectance macrophytes from other similar features such as canopy shade.

Advanced Visible-Near Infra-Red-2 (AVNIR-2) sensor onboard the recently launched ALOS satellite provides data in three visible and one near infra-red bands with relatively moderate spatial resolution and wider ground coverage making it a good choice to address regional scale wetland mapping issues. IKONOS and QuickBird satellites offer the highest resolution data, their per scene area coverage is far less than ALOS (i.e. 2.7% to 5.5% of one ALOS scene respectively). This makes them an expensive choice for regular monitoring of macrophytes at a regional scale, while data captured in small windows in different times of the year can add more complexities in its processing.

Mumby and Edwards (2002) reported user accuracies of mapping seagrass, sand and macroalgae habitats using IKONOS imagery of 89%, 72%, and 60% respectively using spectral and textural information to aid classification. Similarly Malthus and Karpouzli (2003) used supervised classification of 4m multispectral data from the IKONOS satellite which showed overall classification accuracy was 60.3%. Amalgamating sand categories increased overall classification accuracy to 81.0%. Some patches of seagrass were confused with fine sand, probably because the patches of seagrass were both sparse and smaller than the image pixel resolution of 4m. However, the utility of the imagery for classification of bottom habitat on the basis of spectral differences alone was less evident. This highlights the limitation of the three visible and fairly broad bands of IKONOS alone to classify targets such as seagrass and algal species which typically were shown to be relatively dark and with only subtle spectral differences.

Becker et al. (2007) has also highlighted that the band centres of commonly available high-resolution satellite systems are not optimal for differentiating wetland vegetation during the northern hemishpere pre-senescent, late growing season (August/September), particularly in the case of Great Lakes coastal wetlands.

Standard aerial photographs have inherent limitation for detailed wetland mapping due to low spectral information (usually one to three bands) in the image (Jensen et al., 1986). However, recent technological advances have provided high spatial and high spectral resolution (hyperspectral) airborne data, which are better able to match the rich spectral and spatial diversities observed in the aquatic system (Malthus and Mumby, 2003).

Hyperspectral data, if captured over a large region at maximum spatial and spectral resolution, is not only costly but requires more resources and time to store and analyse. However, it is used to optimise the spatial and spectral resolutions to map the Great Lakes coastal wetland using the CASI-2 airborne sensor. Data were acquired with two combinations of spectral and spatial settings i.e. 1-meter resolution imagery with 18 non-contiguous bands and 4-meter resolution imagery with 46 contiguous bands. The research verified that a minimum of seven, strategically located bands (425.4nm, 514.9nm, 560.1nm, 685.5nm, 731.5nm, 812.3nm and 916.7nm) in the VIS–NIR wavelength region (with spatial resolution less than 2m) is necessary to maintain a classification resiliency above the 85% threshold. These seven bands

generated a mildly degraded classification result (13.7% decrease in resiliency) compared to that obtained from full-spectral-resolution (46-band) hyper-spectral imagery (Becker et al., 2007).

Mapping submerged macrophytes along rivers requires another aspect to consider i.e. river size. Small rivers provide difficult conditions for mapping underwater vegetation, because of trees on the riverbanks overhanging and overshadowing the water surface to a large extent. In contrast, large rivers like the Waikato River provide sufficient habitats for submersed macrophytes, and are less covered by bank vegetation (Schulz et al., 2003).

2.4. Remote sensing of limnetic zone

The limnetic zone is the well-lit, open surface waters further from shore in a lake. This area is occupied by a variety of phytoplankton consisting of algae and cyanobacteria as well as zooplankton, small crustaceans, and fish. Most photosynthesis takes part in this part of the lake which is due to the presence of chlorophyll found in the suspended cynobacteria and algae.

There are different water quality parameters that can be detected using optical remotely sensed data. These are chlorophyll *a*, total suspended sediments, secchi depth and water temperature. To determine the temperature of a water body, reflected energy in the thermal infrared part of the electromagnetic spectrum is needed. For other water quality parameters, the data in the optical and near infra-red parts of the electromagnetic energy are required.

The reflectance properties of water are highly dependent on its quality. Clear water reflects little in most spectral regions but it shows the best reflectance in the blue band. The infrared energy is effectively absorbs in the clear water which results in no reflectance in this part of electromagnetic energy (EME). The presence of suspended solids in the water acts as colour producing agents (CPA) which increase the reflectance at visible wavelengths and changes the reflectance peaks from blue light to longer wavelengths. (Valta-Hulkkonen et al., 2003; Verbyla, 1995), therefore multi-band RS data is used to monitor water quality.

Bukata et al. (1997) considers phytoplankton (chlorophyll *a*), suspended minerals (SM) and dissolved organic carbon (DOC) as CPA. Chlorophyll *a* acts primarily as a differential absorber, causing a decrease in the spectral response at the blue to turquoise colour (472-500 nm) of the visible spectrum. Suspended solids are associated with increases in reflected energy at longer red wavelengths (630-690nm). Thus an increase in turbidity (i.e. water containing high concentration of Chl *a* and SM) with a low concentration of DOC displays colours ranging from green to brown (>500nm). Waters with large concentrations of DOC, irrespective of turbidity are invariably shown in a brownish tone (560-570nm).

Chlorophyll *a* concentration and secchi disc depth are used to measure the abundance and variety of these suspended matters in the water. Excessive nutrients can stimulate nuisance algae blooms, resulting in reduced water clarity, reduced amounts of good quality food and depleted oxygen levels in deeper water.

A certain amount of *in-situ* data is needed to find the statistical relationship between the concentration of chlorophyll *a* and the satellite signal. However, these estimates do not have to be collected from every lake under investigation (Pulliainen et al., 2001). The retrieval approach is empirical and requires nearly simultaneous in situ training data on water quality for the determination of regression coefficients. Instead, the results obtained indicate that reliable estimates on the level of chlorophyll-*a* for an individual lake can be achieved without employing *in-situ* data representing this specific lake.

Numerous investigations have shown that strong empirical relationships (such as band ratios) can be developed using visible and NIR data of Landsat Multispectral Scanner (MSS) or Thematic Mapper (TM) imagery and *in-situ* measurements of water quality.

Table 1: Summary of recent remote sensing studies of lake waters using optical imagery

Location	Sensor	Bands	Technique	Variable	Reference
Minnesota	TM, MSS, IKONOS	Blue, Red	Empirical	SEC,CHL, TUR	Kloiber et al., 2002; Lillesand et al., 2004
Norfolk Broads	TM	Blue, Red	Empirical	SEC,TSS, CHL	Baban, 1993
Lake Erken	TM	Green	Chromaticity	TCC, CHL	Oestlund et al., 2001
Lake Garda	TM	Blue, Green, Red	Empirical	CHL	Zilioli and Brivio, 1997
Frisian Lakes	TM & SPOT		Bio-optical modeling	CHL	Dekker et al., 2002
Gulf of Finland	TM		Empirical, Neural Network	CHL, SSC, SEC, TUR	Rogge et al., 2007
Lake Balaton	TM		MNF Transformation, Mixture Modeling	CHL	Tyler et al., 2006
Lake Kinneret	TM	Blue, Green, Red	Empirical	CHL	Mayo et al., 1995
Beaver Reservoir	TM	Blue, Green, Red, NIR	Neural Network	CHL, TSS	Sudheer et al., 2006

CHL – Chlorophyll *a,* SEC- Secchi depth, TUR- Turbidity, TSS – Total suspended sediment

Satellite remote sensing data has been used to detect different forms of chlorophyll *a* sources in the ocean waters. It is important to see whether a particular satellite has the spectral capability to record this information e.g. most of the phycocyanin (present primarily in cyanobacteria) absorption feature is outside band 2 (630-690nm) of Landsat or ALI sensor. Modelling results show that multispectral sensors like ALI, Landsat or MODIS are unlikely to be capable of separating waters dominated by cyanobacteria from waters dominated by the algae species as their spectral band configuration does not allow detecting absorption features caused by phycocyanin. MERIS (300m spatial resolution) bands 6 and 7 allow detection of the phycocyanin absorption feature near 630nm and a small peak in reflectance spectra near 650nm

characteristic only of waters dominated by cyanobacteria. Thus, MERIS can be used in identifying cyanobacteria if they are present in relatively large quantities. Unfortunately it is not possible to use MERIS for early warning of emerging potentially harmful blooms as the minimum biomass needed to cause features in reflectance spectra typical of cyanobacteria is higher than the biomass already considered as a bloom in the Baltic Sea (Kutser et al., 2006a).

2.5. Discussion

Passive or optical remote sensing is undoubtedly a rapid way to gather information for aquatic vegetation studies but it requires a certain amount of time to process the data before inferring the required information. It is true that technological advances like capturing and processing of data have significantly improved our abilities to address environmental issues. The factors that influence the time required for smooth data processing are listed below and discussed in detail. These factors remain a consideration for data processing of regional scale mapping and its regular monitoring, no matter what data processing technique we apply. These factors are:

- Spectral and spatial aspects of the RS data
- Choosing the right platform for RS data capture
- Timing of RS data capture
- Integration of active RS data
- Integrating GIS analysis with RS data analysis

2.5.1. Spatial aspect of remote sensing data

Spatial resolution is the most significant of the many factors that influence the accuracy of land cover characterisation. As described previously, Yang (2007) verified the importance of higher spatial resolution (1-2m) colour aerial images to accurately classify riparian vegetation against SPOT-4 and Landsat-7 ETM+ data. The factor behind the improved classification was spatial resolution of RS data.

In conventional aerial photography, spectral resolution is compensated with high spatial resolution. Nagler et al. (2005) used 50cm spatial resolution oblique and vertical panchromatic (b/w) aerial images to determine different vegetation types in the riparian zone along the lower Colorado River. Their ability to determine different types was limited to texture based feature interpretation for homogeneous growth patches. In mixed growth zones, spectral context may enhance abilities to discriminate between different riparian features.

Maheu-Giroux and Blois (2005) used colour photographs in Saint-Bruno-de-Montarville on the South shore of Montreal, Canada. After scanning at 600 dpi, the resulting pixels had a corresponding ground resolution of 0.33m which proved far superior in enabling the detection of *Phragmites australis* populations compared to the panchromatic images. They suggest that spectral resolution is therefore a determining factor to effectively distinguish different vegetation types.

2.5.2. Spectral aspect of remote sensing data

The ability of optical remote sensing to identify and map any earth surface feature heavily depends on its spectral reflectance i.e. amount of electromagnetic energy reflected after striking with the feature. This is always less than the incident energy as some part of it may get absorbed by the feature or transmitted through it.

This reflectance characteristic is quantified as a function of wavelength and if represented in the form of a graph is known as spectral reflectance curve. The objective of our study is to map aquatic environments, and as a result water and vegetation are the two obvious constituents of our area of study. The reflectance curves of these two feature types are shown in the Figure 4 below.

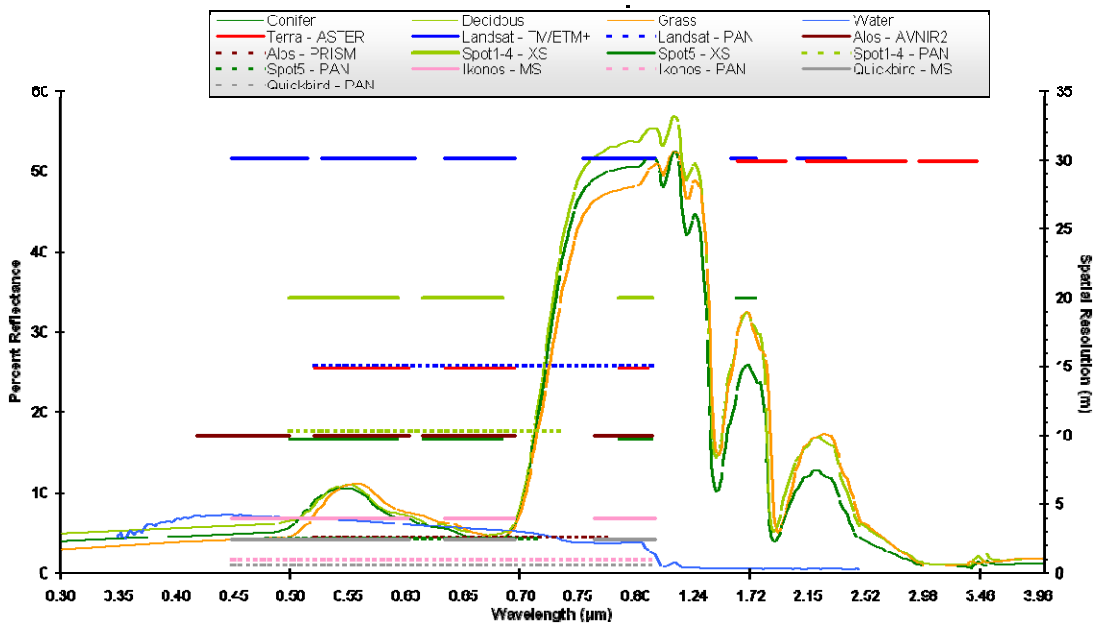

Figure 4: Typical reflectance curves for different vegetation types and open sea water along with the placement of spectral bands for known optical satellite sensors.

To spectrally recognise features in optical RS, data needs to be captured in those spectral bands which show ability to discriminate these features effectively. As discussed earlier, conventional aerial photography is limited to one to three band data which yield poor discrimination of submerged aquatic vegetation if standard data classification procedures are applied. For example, Mount (2006) applied a depth correction factor before fuzzy classifying small format colour aerial photographs which helped in improved classification results for seagrass estimation.

In space borne RS, most of the empirical models use such wavebands which capture data in the visible part by the sensor to calculate water quality parameters such as chlorophyll *a*, suspended sediment concentration (SSC) and coloured dissolved organic matter (CDOM). The data capture in the visible wavebands is also critical to study submerged aquatic vegetation (SAV). In order to map other aquatic vegetation categories such as emergent, floating or riparian, data captured in the infrared wavebands help towards better identification of vegetation due to their higher reflectance peaks than the visible spectrum.

The commercial satellites operate in broad spectral ranges and thus offer less ability to discriminate different features associated with the aquatic habitat. Careful selection of narrow wavebands in aerial remote sensing has shown significant improvement in RS data ability to map coastal vegetation and river water quality (Becker et al., 2005; Becker et al., 2007; Senay et al., 2001). Using this past experience, aerial data in narrow spectral wavebands for the Waikato region may further improve classification accuracies if used in conjunction with advance classification techniques like sub-pixel classifier.

2.5.3. Choosing a remotely sensed data platform

There is no doubt that remotely sensed data is more cost effective than field based assessment. Booth et al. (2007) have estimated that airborne assessment for 770 locations cost around US$ 9000; whereas ground assessment sampled only 60 locations at the cost of US$ 23000. The Tropical Rapid Appraisal of Riparian Condition (TRARC) is a qualitative field based visual assessment method developed specifically for rapid assessment of riparian zone condition in wet-dry savanna environments of tropical Australia. This method was compared with Quick Bird satellite image (Johansen et al., 2007). It was found that for one-off assessments, the field based method was most appropriate at spatial scales from 1km to 200km of river, while the image based method was feasible for mapping riparian areas along 10–2000km of river. Multi-temporal analysis was most accurately performed using the image based method due to the continuous data format.

There are studies that show the effectiveness of aerial photography for aquatic vegetation mapping (Becker et al., 2005; Becker et al., 2007; Booth et al., 2007; Lonard et al., 2000; Maheu-Giroux and Blois, 2005; Malthus and George, 1997; Marshall and Lee, 1994; Nagler et al., 2005; Valta-Hulkkonen et al., 2003; Weber and Dunno, 2001; Whited et al., 2002; Wright et al., 2000). However a study by Yang (2007) shows that the processing of aerial photography takes about 5 times longer than for satellite images. Processing includes ortho-rectification, mosaicing, and classification.

Space borne platforms also offer high spatial and spectral resolution data and global coverage of their data is available in some form continuously from 1972 at varied resolutions. There is no standard costing factor which determines the price for any particular satellite data. There is an element of commercialism and scientific research between different operators that impact on the price of their satellite data. In most of the cases, operating countries or consortia of countries that help in fabricating and launching these satellites offer subsidy for the local use of its data.

High spatial resolution satellite data have been available since 1999 from the launch of IKONOS-2, and its volume increased many fold with the addition of other satellites like QuickBird and OrbView-3. In the near future, there will be more satellites at further improved (0.41m) spatial resolution.

In the case of the Waikato region, one advantage of airborne RS data over space-borne is the impact of local meteorological conditions which cause paucity of data acquisition due to persistent cloud cover. Other factors include the high prices of space-borne data and its temporal (i.e. seasonal) variation. All these factors raise

doubts on the reliability of space-borne satellite data technology for regular monitoring at the regional scale.

2.5.4. Timing of data capture

It is significant to know the timing of data acquisition particularly if the target of observation is vegetation. Phenology is the study of regularly recurring biological phenomena such as leaf blooming during spring to summer and low chlorophyll concentration during fall and winter seasons. For macrophytes, peak biomass is observed during late summer and data captured at that time can play a vital role in discriminating different vegetation types. A seasonal difference in SAV phenology is a contributing factor towards superior classification results as suggested by Wolter et al. (2005).

Davis et al. (2002) used 4 band (visible to near infra-red) multispectral aerial data to determine different riparian habitat. They have suggested that classification accuracies for the riparian vegetation units in the Grand Canyon do not appear to be influenced by season of data acquisition, although data acquired under direct sunlight produced higher overall accuracies than data acquired under overcast conditions. The latter observation, in addition to the importance of band reflectance for classification, implies that data should be acquired near summer solstice when sun elevation and reflectance is highest and when shadows cast by steep canyon walls are minimised.

A very similar situation exists in the Waikato region where overcast of the surrounding riparian trees can impact negatively on the submerged aquatic vegetation if data is captured during low solar elevation.

2.5.5. Integration of active sensor data with optical data

Remote sensing is clearly divided into broad categories based on its ability to capture data. Optical remote sensing utilises available energy coming from the sun to capture data and works in the short wavelength (ranging between 0.4 to 12.0µm i.e. visible to thermal infra-red) part of the electromagnetic energy (EME) spectrum. Passive optical imagery is much more effective for mapping bottom type in clear, shallow (up to ~ 20 metres) waters. It is useful not only for delineating the extent and distribution of different bottom types, but also makes it feasible to monitor habitat change (Davies and Merton, 2007).

On the other hand, active RS systems carry their own source of energy that is emitted in a well defined wave length range which could be in the ultraviolet to near infra-red part (known as LIDAR) or microwave part (known as RADAR) of EME. This is in contrast to light sources such as the incandescent light bulb, which emits over a wide spectrum of wave length.

In microwave sensing, the image of the surface is generated by emitting high energy pulses of microwave, which when reflected from the surface features, (called reflected signal or echo) are returned to the sensor. These echoes are processed to determine the distance of the target, and information is recorded in a digital number like an image for further analysis. Microwave sensing has a distinct advantage over conventional optical RS as it can penetrate through clouds, haze and fog thus making it an obvious

choice for mapping tropical regions which remain under persistent cloud cover during the year.

For microwave sensing, flat water surface acts as a high reflectivity medium and yields no echoes to the antenna. Thus it provides no utility for determining submerged aquatic vegetation. However it showed improvements in mangrove classification from 67% to 76% accuracy based on classification of integrated optical and SAR data which improved further to 80% using a neural network classification (Held et al., 2003).

In LIDAR sensing, the use of rapidly pulsing (ranging between 20,000 to 50,000 pulses/sec) laser light (i.e. a light in a narrow, low-divergence beam and with a well-defined wavelength or colour if the laser is operating in the visible spectrum) is directed towards the ground and the time of pulse return is measured. The return time for each pulse is processed to calculate the variable distances between the sensor and various surfaces on (or above) the ground. Modern systems are able to record up to five returns per pulse (Lillesand et al., 2004). In multiple-return lidar systems, the first return measures the elevation of building roofs or tree canopies. Multiple returns discriminate intermediate forest structures and under-storey plantation as well as submerged plant heights in case the first return is from open surface water. Following the initial processing, lidar data is prepared as a file of x, y, z points. Relatively accurate data of a river corridor is achieved at point densities between 50,000 to 100,000 points per km^2 which is not feasible with other survey technologies (Bowen and Waltermire, 2002). Unlike Radar systems, Lidar systems operate in the optical range and are thus subject to interaction with clouds and other atmospheric constituents (Vis et al., 2003).

Acoustic systems are the standard for bathymetric mapping in deeper waters (Davies and Merton, 2007). They use SONAR technology to create a pulse of sound (or an acoustic wave) with the help of an echo sounder, and then listen for reflections (echo) of the pulse. Acoustic Ground Discrimination Systems (AGDS) are relatively cheap and easily integrated with standard survey vessel hardware like echo sounder and geographical positioning system and are able to quickly produce coarse resolution data. Mapping with AGDS can generate similar imagery to satellites without the restrictions of water penetration and obstruction from cloud (White et al., 2003; Wilding et al., 2003). This appears to fill a gap in the inventory of established methods for submersed macrophytes (Sabol et al., 2002; Valley et al., 2005).

2.5.6. Integration of GIS analysis with RS data processing

Due to the richness of the data from remote sensing images, GIS represents an effective environment for the maintenance and exploitation of data (Caloz and Collet, 1997). In addition to this, GIS has the potential for advanced analysis and modelling abilities which are limited in remote sensing tools (Yang, 2007). More importantly, these spatial analysis processes can be automated in such an environment using scripts (such as AML – Arc Macro Language) so that they are repeatable and easy to operate.

GIS can be used for map presentation and query for some end users. Yang (2007) used GIS as an integrated environment to RS for data storage, preparation, and analysis for riparian vegetation delineation and mapping at all stages of data

processing. He further recommended that riparian vegetation is better mapped using sectional polygons for large scale (in detail) maps and linear representation for small scale (large area) maps.

Chapter 3

Available RS Data and its Processing for Waikato Region

One of the objectives of this study is the trial processing of satellite data for at least one site in the Waikato region to assess its effectiveness. This assessment shall be refined further using advance image processing techniques to monitoring habitat characteristics for riparian, littoral and limnetic zones of large rivers and lakes of the Waikato region. This preliminary trial assessment exercise has three sections:

a. To identify RS data which is available or can be made available for the entire region in a cost effective way,
b. To identify suitable data processing techniques which are replicable in order to establish RS as a tool to monitor aquatic parameters on a regular basis and;
c. To identify field activities which are required in parallel to validate and improve RS data processing.

This chapter thus provides an overview of the research approach and provides summaries of the study area, potential data sets and a review of different data analysis techniques.

3.1. Study area

This study aims to ultimately monitor the riparian and littoral vegetation along large rivers and lakes of the Waikato region using remotely sensed data. Waikato means "flowing water" in Maori language and the Waikato River is the longest river in New Zealand. It originates 2797 metres above sea level from the eastern slopes of Mount Ruapehu. Before entering into NZ's largest lake, Lake Taupo, it is known as the Tongariro River for part of its length. On leaving Lake Taupo, the river cuts through the volcanic plateau flowing north, passing through eight hydro-electric dams before reaching the flat plains of the middle Waikato basin or Hamilton lowlands. The river's main tributary is the Waipa River which flows for 115km and confluences with the Waikato at Ngaruawahia. After the confluence, it passes through the Taupiri Gorge and reaches the flat country of the lower Waikato before entering into the Tasman Sea at Port Waikato. The Waihou and Piako Rivers are the other two main rivers of the Waikato region and run through the Hauraki Plains. The Waihou River flows for 150 kilometers before reaching the Firth of Thames at the south end of the Hauraki Gulf near the town of Thames. The length of Piako River is 100 kilometers and drains some 4 km west from the mouth of the Waihou River in the Firth of Thames.

There are over 100 lakes in the Waikato Region, which vary considerably in their physical, chemical and biological characteristics. The lakes can be grouped spatially by their geographic association; the Taupo volcanic zone lakes, West Coast dune lakes, Waikato hydro-lakes, Waikato peat lakes, and the lowland Waikato riverine lakes. The majority of the region's lakes are shallow and less than 10 hectares in size. The intense sediment-water interaction and the potentially large impact of aquatic

vegetation makes the functioning of shallow lakes different from that of deep lakes such as Lake Taupo or the Waikato hydro-lakes (Barnes, 2002). Over the last one hundred years, lakes in the Waikato region have undergone marked changes at an unnatural rate and many have now become de-vegetated. Major factors causing the accelerated decline in ecological condition of lakes in the Waikato region include declining water quality and introduction of invasive fish and plant species.

3.2. Availability and identification of remote sensing data

There are over 30 RS satellites currently operational, however many of these can not be easily accessed because of the following factors:

i) Product quality (already discussed before in Chapter 1),
ii) Value-added/derived products,
iii) Catalogue of images and query based data search system,
iv) Programmability to acquire data and its delivery time, and
v) Program continuity.

Most commercially orientated satellite operators offer an online mechanism to launch data acquisition requests or have extensive commercial partners' networks to collect orders for new tasking. Most of the RS satellites operate in near polar orbits which enable data capture for the entire globe; however some satellite operators provide data for their limited area thus the usefulness of RS data is subject to its availability.

Of the available RS data, identification of appropriate data for any specific area or region needs to consider some additional factors. These factors are usually associated with the ground situation and are summarised as:

vi) The size of the study area,
vii) Meteorological (weather) condition of the region,
viii) Seasonal variations (in the case of more than one dataset etc.), and
ix) Cost of the RS data.

The size of the study area matters the most. Keeping in view the space-borne data geometry, these satellites fly over the earth from north to south. That way, the width of the study area is more critical than its total area. For example, the Waikato region is roughly 165km wide and 315km long in its extent. To cover this region using Landsat TM data (knowing that its data extent is 185km x 185km), it may need two along-track images to cover the entire Waikato region. However, these satellites follow a predefined path which does not necessarily match with the width of the study area. Some satellites are capable of side-view scanning which enable them to cover the missing part of the AOI in the east or west direction. Landsat TM sensor is not capable of side-view scanning thus requires a minimum of two side by side strips of data to cover the entire Waikato region. For satellites that lack side-viewing capability, temporal resolution becomes significant in order to determine data availability for the adjacent passes. In case of Landsat, minimum offset for the adjacent pass is 7 days.

The metrological condition of any area can add more complexities. The visible and infrared wavelength of the energy spectrum does not penetrate through clouds thus presence of cloud is a significant data quality eroding factor. In the case of Landsat, if

there is cloud on an area adjacent to its previous path then the next pass over this region will not happen before 16 days. If the purpose of data capture is to monitor nuisance algal blooms in lakes, there will be 24 days offset between two adjacent images, if the satellite fails to acquire data on the first pass.

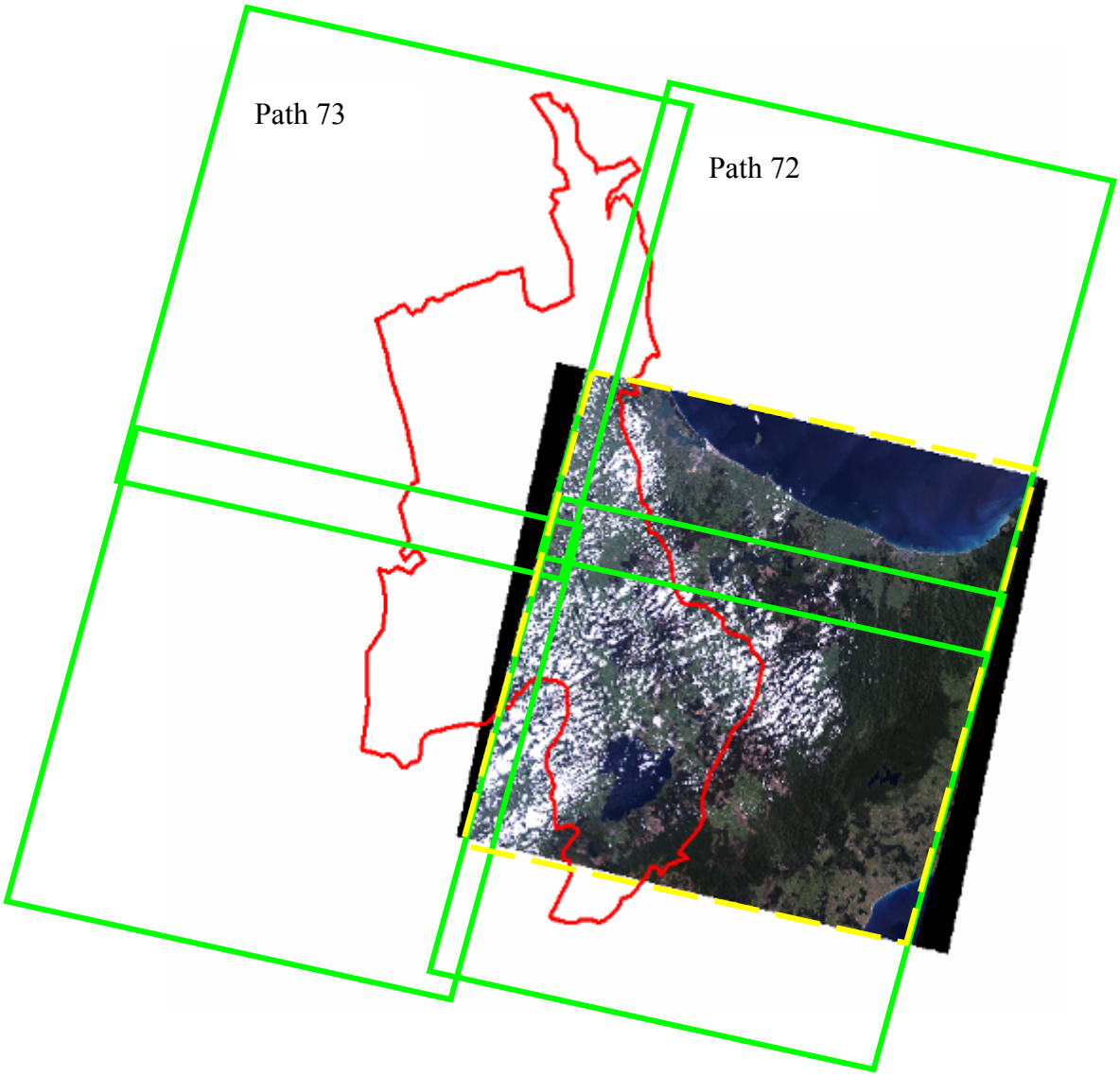

Figure 5: Landsat data swathe over Waikato region showing individual scenes in green boxes. The yellow box indicates the satellite data with 60% along track shift, acquired on 30th Jan 2007.

High resolution satellites usually acquire data in narrow swathes (from 11 to 16km), thus data are acquired after multiple passes over the larger region. In the case of IKONOS images, which have data swathes of 11 kilometres, it can not acquire data for the entire Waikato region in less than 15 different dates. Luckily these satellites have pointing angles, but require a minimum of 4 days to fly over any region. This means that one time acquisition for the entire Waikato region will take a minimum of 60 days, provided that no single passes over the region are obscured due to cloud. Such a wide time difference can intensify certain seasonal variations. For example, a change in plant phenology makes it harder to classify vegetation with the same level of confidence across multi-seasonal images.

If comparing different available RS data sources for this study, these datasets very clearly fall into four distinct categories based on their data swathe. These categories are:

- Narrow swathe RS data up to 25km range: This group includes data from EO-1 Hyperion – 7.7km; OrbView3 – 8km; WRAPS contact prints – 9.2km; IKONOS – 11km; PROBA CHRIS – 14km; QuickBird – 16km, ResourceSat LISS-IV (multispectral mode) – 23km etc.
- Medium swathe RS data up to 100km range: This group includes satellites and sensors such as ALOS PRISM – 35km; EO-1 ALI – 37km; SPOT & ASTER – 60km; ALOS AVNIR2 – 70km; Monitor-E-1 PAN – 94km etc.
- Large swathe RS data up to 300km range: Main satellites in this group are limited to CBERS-2 – 113km; IRS and ResourceSat LISS-II & -III – 140km; Monitor-E-1 multispectral – 160km and Landsat 185km.
- Very large swathe RS data above 500km range: Mostly satellites in this group have very large swathe data acquisition capability which normally starts above 500km width. At this moment, this group is limited and only DMC series satellites and the ResourceSat AWiFS sensor provide 32m and 56m multispectral data at 600km and 740km wide swathes. Other sensors in this category possess low spatial resolution.

Meteorological data for any region usually include sunshine hours which can be used as a good indicator to asses overall cloud cover for the region. It is however important to note that most of the satellites pass over any particular latitude between 1000 to 1200 hours local time. Acquisition of airborne data happens usually between 1100 to 1300 hours local time when the solar elevation is higher to avoid sun glitter. Thus the total number of sunshine hours on a monthly basis does not reveal information about cloud cover particularly for that part of the day in which RS data is usually acquired. The sunshine data for Hamilton city indicates that the best time for acquisition of data was between December 2006 and March 2007 when average per day sunshine remained above 6 hours. Data captured during this season also fit in with the time of low flows in rivers and highest macrophyte biomass.

Table 2: Sunshine hours for Hamilton city

Month	Sunshine (hours)	Ave. sunshine per day (hrs - min)	% of normal sunshine	Remarks
Oct 2006	144	4 hrs 39 min	82	Below normal
Nov 2006	143	4 hrs 46 min	72	Well below normal
Dec 2006	218	7 hrs 02 min	98	Near normal
Jan 2007	190	6 hrs 07 min	82	Below normal
Feb 2007	196	7 hrs	99	Near normal
Mar 2007	180	5 hrs 49 min	97	Near normal
Apr 2007	160	5 hrs 20 min	98	Near normal
May 2007	123	3 hrs 58 min	94	Near normal

Source: (NIWA-Science, 2007)

If more than two compatible datasets from different sensors are available then the cost of data is perhaps the last element to consider. However it is perhaps the most critical part during the planning phase. For example, high resolution satellite data like QuickBird's 0.6m resolution panchromatic data cost around NZ$19 per km^2. Its multispectral data costs the same if purchased separately. However, if it is acquired as

a bundle (i.e. panchromatic and multispectral), both the datasets cost NZ$23 per km^2 in total. SPOT and ALOS do not offer the facility of bundled acquisition for their panchromatic and multispectral images. Certain image processing techniques can fuse low resolution multispectral data with high resolution panchromatic (i.e. black and white) data to make high resolution multispectral images. This way SPOT and ALOS data can be viewed and classified at 2.5m resolution which costs considerably less than buying multispectral data of QuickBird alone. Table 3 shows the unit cost per km for different satellites along with options that deal with flexibility for data purchase.

Table 3: Unit cost of RS data for different satellite sensors along with options to buy archived data or conduct new acquisitions

Satellite / sensor	Mode	Archived scene cost (NZ$)	Scene area (Km^2)	Unit cost per km^2 (NZ$)	Sub-scene avail-ability	Along-track		New tasking flexibility
						Scene shift Adjust-ment	Multiple scene subsidy	
Landsat TM	Bundled	1350	34225	0.04	☹	☺	☺	*
Spot-5	PAN	5800	3600	1.6	☺	☺	☹	☺
	Multi	5800	3600	1.6	☺	☺	☹	☺
	Bundled	11600	3600	3.2	☺	☺	☹	☺
Spot-4	PAN	4250	3600	1.18	☺	☺	☹	☺
	Multi	4250	3600	1.18	☺	☺	☹	☺
	Bundled	8500	3600	2.36	☺	☺	☹	☺
Terra ASTER	Bundled	135	3600	0.038	☹	☹	☹	☺
EO-1 ALI	Bundled	525	6845	0.077	☹	☹	☹	☺
EO-1 Hyperion	Bundled	525	1425	0.37	☹	☹	☹	☺
Quickbird	PAN	5150	272	19	☺	☹	☹	☺
	Multi-	5150	272	19	☺	☹	☹	☺
	Bundled	6250	272	23	☺	☹	☹	☺
IRS-6P LISS-IV	PAN	2700	4900	0.55	☺	?	?	☺
	Multi	2700	529	5.1	☺	?	?	☺
IRS-6P AWiFS	Multi	2700	547600	0.005	☺	?	?	☺
DMC satellites	Multi	5100[a] 24730[b]	300000	0.023 0.082	☺	?	?	☺
ALOS	PAN	375$^+$	4900	0.076	☹	☺	☹	?
	Multi-	375$^+$	4900	0.076	☹	☺	☹	?
	Bundled	750$^+$	4900	0.153	☹	☺	☹	?

☺ = Yes; ☹ = No; ? = Not sure

* It is assumed that Landsat TM data is captured on every pass

\+ Non-commercial price (commercial cost is ~ NZ$ 1100)

a, b for archive data less than and more than 90 days old respectively

Table 4 summarises different data quality, availability and processing factors which can contribute towards the selection of RS data to carry out the current study.

Table 4: Sensor wise review of different data quality, availability and processing factors

Satellite Sensor	Resolution				Archive	Cost	No of scenes*	Ease of data Processing	Data continuity
	Spatial	Spectral	Radio-metric	Temporal					
Landsat TM	☹	☺	😐	☹	☺	☺	☺	☺	😐
EO-1 ALI	😐	☺	😐	☹	☹	☺	☹	😐	☹
EO-1 Hyperion	☹	☺	😐	☹	☹	☺	☹	☹	☹
Spot-2, 4	😐	😐	😐	☺	☺	😐	☺	☺	☺
Spot-5	☺	😐	😐	☺	☺	☺	☺	☺	😐
Terra ASTER	☹	☺	😐	☹	😐	☺	☺	☺	☹
IRS-6P LISS-IV	☺	😐	☺	😐	😐	☺	☺	☺	☺
DMC Sat	☹	😐	😐	☺	😐	☺	☺	☺	☺
ALOS	☺	☺	😐	☺	☹	☺	☺	☺	😐
IKONOS	☺	☺	☺	😐	😐	☹	☹	☹	☺
QuickBird	☺	☺	☺	😐	😐	☹	☹	☹	☺
Multispectral aerial photos	☺	☺	☺	☹	☹	😐	😐	☹	☺

* indicates ease of data capture

☺ Meets requirement; 😐 satisfactory but not preferred; ☹ doesn't meet requirement.

Based on the above assessments for data quality, its acquisition and processing, Table 5 below summarise different attributes that can be summarised by these different sensors.

Table 5: Sensor wise review of different data quality, availability and processing factors

Satellite Sensor	Riparian	Aquatic Vegetation		Water Quality		
		Submerged	Emergent	Chl a	Turbidity	Temp
Landsat TM	😐	😐	😐	☺	☺	☺
EO-1 ALI	☺	😐	☺	☺	☺	☺
EO-1 Hyperion	😐	😐	😐	☺	☺	☺
Spot-2, 4	☺	☹	😐	😐	😐	☹
Spot-5	☺	☹	☺	😐	😐	☹
Terra ASTER	😐	☹	😐	😐	😐	☺
IRS-6P LISS-IV	☹	😐	😐	☺	☺	☹
DMC Sat	😐	☹	☹	😐	😐	☹
ALOS	☺	☺	☺	☺	☺	☹
IKONOS	☺	☺	☺	☺	☺	☹
QuickBird	☺	☺	☺	☺	☺	☹
WRAPS photos	😐	☹	😐	☹	☹	☹
Multispectral aerial photo	☺	☺	☺	☺	☺	☺

☺ Meets requirement; 😐 satisfactory but not preferred; ☹ doesn't meet requirement.

There are two initiatives at a regional and national level which offer good opportunities to make available regional scale RS data at nominal cost for monitoring different aquatic habitats.

3.2.1. WRAPS initiative

WRAPS stands for Waikato Regional Aerial Photography Syndicate. Its first regional scale data was captured in 1993. WRAPS 2002 is the latest and complete series which was flown in 2001/02 summer for most of the region except for Coromandel Peninsula and Lake Taupo (Oct 2002). Its complete dataset contains approximately 3200 digital orthophoto tiles covering the entire Waikato Region. In June 2006 Coromandel Peninsula and Firth of Thames estuary were surveyed in order to upgrade WRAPS inventory. Unfortunately for other regions, aerial photography has been postponed due to the consistently bad meteorological conditions (such as persistent cloud cover) during last summer. The remaining parts of the region will be covered during the end of 2007.

The 24-bit colour aerial photography was flown at 20,000 feet with zero cloud cover and a sun angle of ≥ 40 degrees. A LH Systems RC 30 camera with 152mm focal length was used. Using the equation 1 in Appendix A, these specifications produced a contact print scale of 1:40,000, held by EW. These aerial photographs were scanned at 12.5μm (0.5m resolution) and then resampled to 1.0m final resolution. The digital ortho-photos are designed to be used at a maximum scale of 1:5000. Its horizontal accuracy is ±3 metres at 90% confidence. Each image was corrected for lens distortion, image tilt and terrain distortion by using a high order photogrammetric orthophoto process. Each digital orthophoto covers an area of 2,400m east west (EW) and 3,600m north south (NS). Under WRAPS 2006 the same equipment, data acquisition and processing techniques are used. However, this time aerial photos are resampled at 0.625m instead of 1m.

3.2.2. All of Government (KiwImage) initiative

In 2004 the *Officials Committee on Geospatial Information* (OCGI) set up a subcommittee to talk about the possibility of government level purchase of satellite imagery. A key point was that the imagery had to be available to any central or local government agency. The group received responses covering more than 20 needs. Based on the needs analysis, DigitalGlobe's QuickBird satellite data will be acquired for this initiative. The initiative hopes to be able to capture panchromatic, natural colour and multi-spectral imagery for all of New Zealand within a 5 year time frame.

Final costing of this project is not known but the proposed business plan suggests that EW can pay NZ$15,000 per annum and can fully use this data for its planning. QuickBird offers highest spatial resolution imagery and is ideal to study heterogeneous environments, however the seasonal variations within multi-date images can impact negatively on its full utilisation for aquatic habitats mapping. Such studies require updating of information on yearly bases whereas *KiwImage* would require 2 to 3 years to capture one time dataset the entire region. Despite this fact, these datasets may provide a good opportunity to establish baseline extent mapping for riparian and littoral zones.

3.2.3. Development of multispectral modular camera for aerial data

The significant limitations associated with RS data acquisition under WRAPS and KiwImage are low spectral sensitivity for colour film and plausible seasonal mismatch between different images respectively. It is high time to remodel the existing culture of photographic film based acquisition with true digital photography in discrete multispectral bands.

Digital aerial cameras have a major share in the RS data market when it comes to ground resolutions of well below 1 meter. For photogrammetric applications, digital aerial cameras have to fulfil high demands. The main advantages of digital aerial cameras over their analogue counterparts are a completely digital data flow line, a significantly improved radiometric image quality, together with the possibility to simultaneously acquire panchromatic, colour and near-infrared imagery (Heipke et al., 2006).

It is difficult to assess how many digital cameras are available in the market but Graham and Mills (2000) noted that by 1996 only 40 digital cameras of commercial and industrial use were available. This increased to more than 200 in 1997. This exponential rise has impacted on the utilisation for aerial imaging as well. By May 2006 (as researched by Professor Gordon Petrie of Glasgow University), approximately 120 high-end or "large format" systems (Leica ADS40, Intergraph DMC, Vexcel Ultra-Cam-D), as well as around 150 "medium format" cameras plus many more "small format" solutions, are reported to be in operation world-wide (Heipke et al., 2006).

Many environmental (not photogrammetry level) applications have successfully reported the use of small frame digital cameras for riparian and littoral mapping (Booth et al., 2006; Booth et al., 2007; Davis, 2002; Davis et al., 2002; Lieng et al., 2003; Nagler et al., 2005; Wright et al., 2000). Some of them have used very simple methods to cheaply acquire airborne RS data. Examples of these approaches are discussed below.

Nagler et al. (2005) used a single-engine Cessna with vertically mounted Nikon D1 digital camera, flown 1000m above ground level (AGL) at 90 - 100 knots in a grid pattern over the area of interest which captured 15 jpeg photos per minute from the camera into a laptop computer. A separate laptop computer was used to electronically snap the camera shutter and to record the GPS coordinates and acquisition time of each photo using specific software developed for this application. The camera was fitted with a wide angle lens having a field of view of 1000×660m fore-and-aft when flown at an altitude of 1000m AGL. A 500m interval between photos was used (24% overlap). Each camera image contained approximately 2.7 mega-pixels for a spatial resolution of approximately 0.5m without the support of gimbal which resulted in distorted images according to the pitch, roll and yaw of the aircraft. A gimbal is a mechanical device consisting of two rings mounted on axes at right angles to each other so that objects on it remain suspended in a horizontal plane between them regardless of any motion of its support to ensure that pictures are taken in the same orientation and at a nadir angle. To overcome the inherent distortion, these images were individually placed on an existing USGS orthophoto base map in Adobe Photoshop software. Each photo was scaled, oriented and linearly warped to produce good agreement between the location of objects on the photo and the same objects on

the base map. Thus a photo-mosaic was constructed from 148 vertical photos. The resulting colour mosaic inherited the positioning accuracy of the original USGS photos. During the flight an observer collected a continuous (overlapping) set of oblique colour images of the refuge through the airplane window, with a high resolution film camera. These were correlated by picture number with written commentary on the identity of plants on the ground as viewed from the airplane. These additional data were used to refine the plant identifications on the vertical photos at a later stage.

Booth et al. (2006 & 2007) used very large scale aerial (VLSA) images (2cm spatial resolution) to systematically sample an area of interest by acquiring numerous images at intermittent intervals over the survey area and its subdivisions (stream reaches). They suggest that VLSA survey is not intended to accomplish riparian mapping because it is intermittent sampling across extensive landscapes as opposed to continuous photographic coverage. To acquire VLSA images, they used a light airplane (225kg empty weight, fixed wing), a navigation and camera-triggering system, a digital camera, and a laser rangefinder. They used a Canon EOS 1DS 11.1-megapixel single lens reflex, colour (RGB) digital camera with a Canon 100mm f/2.8 EF USM lens. The camera interfaced with a laptop PC running Canon Remote Capture software and images were stored directly on the 40 GB laptop hard drive. A Riegl LD90-3100VHS-FLP laser distance meter was used as an altimeter in conjunction with LaserLOG software (Booth et al., 2006) to continuously read and record the airplane's altitude above-ground-level (AGL) below 300m. Altitude was displayed for the pilot on the laptop screen, while stored data were saved for later correlation with images. Flight altitudes at image capture ranged from 150m to 300m AGL, resulting in image resolutions of 1.3cm to 2.6cm GSD.

As discussed in Appendix A, conventional photogrammetric mapping is based on 23cm × 23cm large-format film cameras. Muller (1997) suggests that an array of 21000 detectors would be necessary to retain the spatial integrity of large format films. The production of sufficiently large CCD arrays is impossible at the moment, so large-format digital cameras are built either as multi-head systems by fusing several smaller CCD arrays and cameras, or by using linear CCD arrays (Honkavaara et al., 2006).

Graham and Mills (2000) have described minimum specifications required for a single area array digital camera that can be used for mapping, GIS and remote sensing. Following characteristics are suggested:

i) A frame format of 100 x 100mm or larger,
ii) A single area array digital sensor with options for monochrome, colour and CIR (colour infrared) versions,
iii) A sensor resolution of 10μm pixel size (i.e. 100 mega-pixel for 100mm x 100mm array),
iv) A minimum frame download period of 3sec/image or better,
v) High geometric quality lens with focal length from 20mm to 50mm,
vi) Shutter speed ranging from 1/100 to 1/2000 sec,
vii) Sensor sensitivity ranging from 100 ISO to 800 ISO,
viii) GPS and intervalometer (a device to trigger exposures of a camera at a defined interval) interface capability, and

ix) Edge of frame data recording facility.

Lockheed Martin's Fairchild Systems have reported the fabrication of 9216 x 9216 pixels array (~85 mega-pixel) of 8.5µm pixel size (Mathews, 1998). DALSA Corporation, an international high performance semiconductor and electronics company, successfully fabricated and delivered the world's highest resolution image sensor chip for astronomical applications in June 2006. This CCD device measures approximately four inches by four inches and has a total resolution of over 111 million pixels (10,560 pixels x 10,560 pixels at 9µm). It is the world's first imager to break the 100 mega-pixel barrier. However, commercially available cameras like Canon EOS 5D (launched in 2005) offers 12.8 mega-pixel images and has only 35.8mm x 23.9mm frame format with 8.2µm pixel size. Besides the CCD array size and its resolution, all the other characteristics suggested above are usually attainable.

In order to capture RS data for EW to study aquatic habitats, we need to understand that this proposed camera model is not an alternate to WRAPS initiative nor can it overtake the KiwImage initiative as both have multiple levels of data utilisation. The purpose of establishing a local aerial data capture module is to bring cost effectiveness with the right kind of spatial and spectral resolution, and to set off hassle-free processing of regularly captured high resolution data for narrow margins of large rivers and lakes of the region.

There are two possible models that can be considered. A dichroic prism based approach can record 3 to 4 images simultaneously using only one camera. Such multispectral cameras are available in the market, for example the MS4100 by Geospatial Systems Inc. This camera can provide a 6.2 mega-pixel image in 3 discrete spectral bands in colour (as blue, green, red) or colour infrared (as green, red, near infrared) formation and costs around NZ$27,000. The manufacture of such cameras requires extensive laboratory calibrations for spectral response. As a result, modification in spectral responses is not possible.

Figure 6: MS4100, a 3-CCD array camera manufactured by Geospatial Systems Inc.

A modular approach with a minimum set of 4 cameras using synchronised trigging function can generate multispectral data. A customised camera with *software development kit* (SDK) (such as the Lw259 USB camera) costs around NZ$5000. This camera carries a CCD array with 1920 x 1080 pixels with pixel size and bit depth of 7.4µm and 12 bits respectively. A combination of four such cameras with band-pass filters can easily record change in the spectral responses according to the nature of local flora to be detected. It can be experimented with a camera to take four sorties over the same area with band adjustments between flights. In overall design, such an approach is easy to fabricate and costs less than 3-CCD array multispectral camera. If this camera is flown at an altitude of 1000m with a standard 35mm focal length lens, it will generate an image with 0.205m GSD while the image size will be 395m by 222m. An aeroplane at the speed of 180km/h (~100 knots) can capture 15 images per minute to ensure enough overlap for data continuity. The overall images required to cover the entire length of the Waikato River will not exceed 2000 images in number.

Figure 7: Lw259 series camera manufactured by Lumenera Co.

Acousto-Optic Tunable Filters (AOTF) are new type of band-pass filters which can be tuned to different wavelength ranges for the incoming light in a quick succession. An Acousto-Optic Tunable Filter (AOTF) camera adapter such as shown in the Figure 8 is software based programmable device which can be plugged in between camera body and an optical lens. Such filters can capture data up to 8 different user defined spectral modes (ranging from 0.4µm to 1.0µm) in one second. Integrating this device will maintain the low cost fabrication of a multispectral camera.

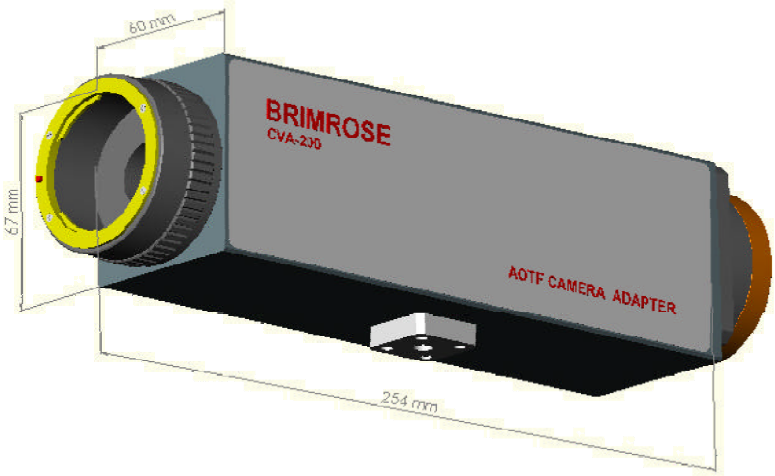

Figure 8: CVA200 series AOTF camera adapter manufactured by Brimrose Co.

In order to stabilise cameras from 3-axis flight motion variations (i.e. roll, pitch and yaw), a gyro-stabiliser or vertical aerial mount gimbal is an important component of the design, and range in price up to NZ$6000.

3.3. Selection of remote sensing data for the trial study

The current study requires the trial processing of RS data. This includes vegetation classification for the riparian and littoral zones and water quality modelling for the open water bodies. Recently captured images from different satellite sensors were searched including archive data for Landsat, ALOS, QuickBird, EO-1 and IKONOS satellites. Sensors onboard these satellites capture data in the blue wavelength that exhibit maximum penetration in the water.

Originally Lake D (situated in the north of Hamilton) was discussed as a potential area for trial assessment. Options for conducting aerial photography for the trial assessment site were also investigated. For the aerial photography, TerraLink and NZ Aerial Mapping (or GeoSmart) are two leading sources. They prefer to undertake larger areas, particularly TerraLink who are involved with EW with WRAPS image acquisition using large frame film plate Leica RC-30 camera. Such cameras are not very cost effective for limited quantity or one-off aerial photography. For this purpose, the Hamilton based company *Lyfestyle Research Ltd / LAP 2003 Ltd*, was contacted. They were interested in experimenting with simultaneous acquisition of aerial photographs for Lake D using colour and black and white IR films. The idea was to fuse or merge both images to generate a pseudo multispectral image for trial classification of different vegetation types. However local climatic conditions did not permit aerial photography to be conducted during the months of March and April 2007.

Data archives for different satellites showed there had been some effort by the ALOS satellite to capture data for the Waikato region from Dec 2006 to March 2007 but it failed to capture any cloud free images for the northern Waikato. EO-1 captures data only on request basis so its archived data did not contain any images over Hamilton and the Lake D area. Of the high resolution satellites, IKONOS satellite has data for this region in its archive but it is five years old. There have been no significant attempts to refresh its data inventory, possibly because its data has not been extensively used in the past.

QuickBird satellite has made consistent efforts on a yearly basis to capture a one time cloud free image for the entire Waikato region. In the six years since 2002, roughly 75% cloud free images of the entire Waikato have been captured. Unfortunately Lake D is not included in its current archive.

It was also reported that NZ Aerial Mapping had brought in CASI-2 sensor in 2004. Hyperspectral data for a few lakes of Waikato and Bay of Plenty were captured to show the usefulness of this data to NIWA. For some reason, this data has not been utilised by them and the whereabouts of it is unknown.

A search through the archives of the ALI and Hyperion sensors onboard EO-1 satellite revealed that there is only one image available for the Waikato region. The geographical extent of ALI sensor (37km swathe) covers the Hardcastle lagoon on the

Waikato River. Although the data coverage of Hyperion sensor (7.7km) was fully lying within ALI data extent, it did not include the Hardcastle lagoon. Thus it was not considered a viable option for the trial assessment.

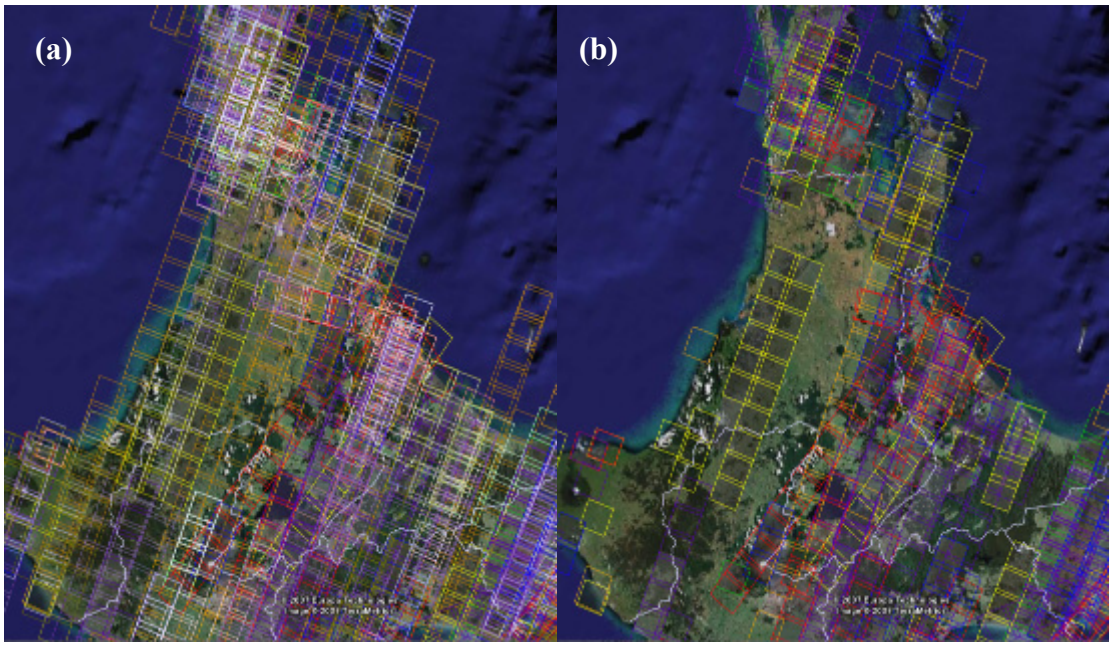

Figure 9: (a) All data archived for QuickBird over the Waikato region, and (b) the extent of low cloud cover (0 to 10%) images

Eventually the southern end of Lake Taupo was selected as good site for a trial assessment. This site includes a good representation of riparian vegetation along the Tongariro River banks where it meets the lake and was reported to have a good coverage of native and invasive macrophytes.

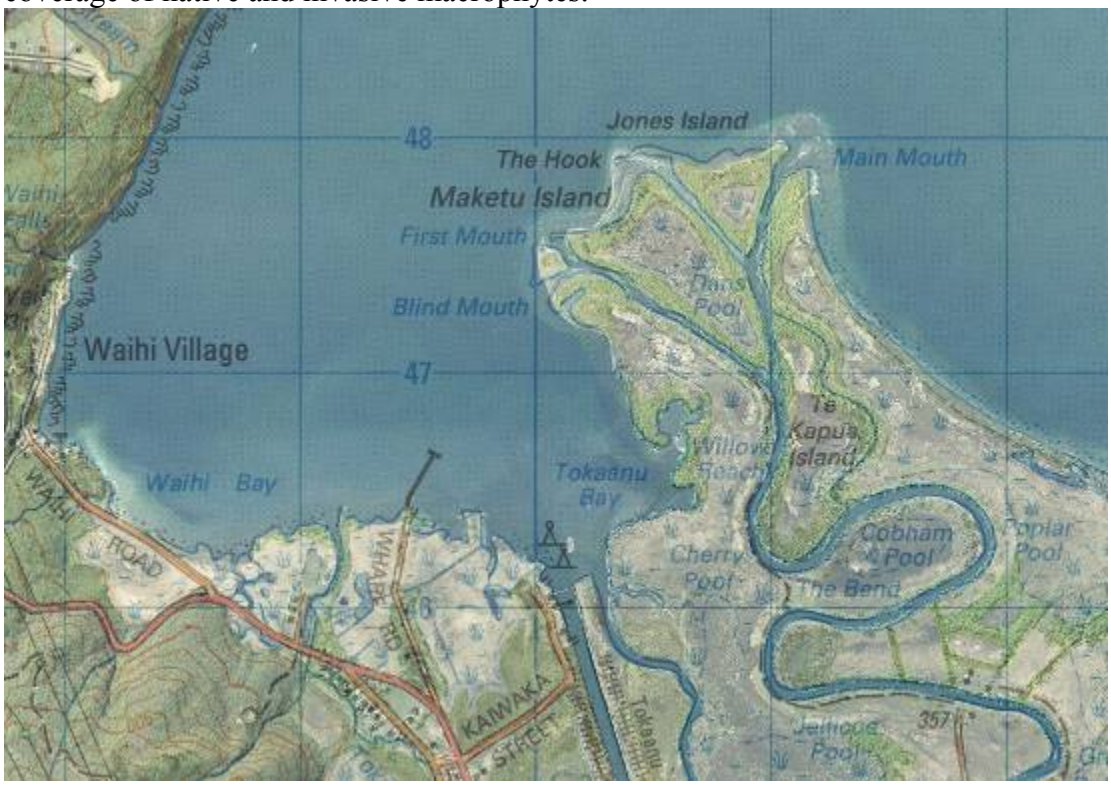

Figure 10: Map of study area showing topographic map sheet draped over the aerial image

Figure 11: Aerial image (WRAPS) captured on October 2003 shows the littoral and riparian vegetation in the study area

Landsat, ALOS and QuickBird satellites also captured this area during last summer with a time difference of less than 4 months and thus there was a good opportunity to use these data for sub-pixel classification.

Figure 12: Landsat image of the eastern Waikato captured on 30th Jan 2007.

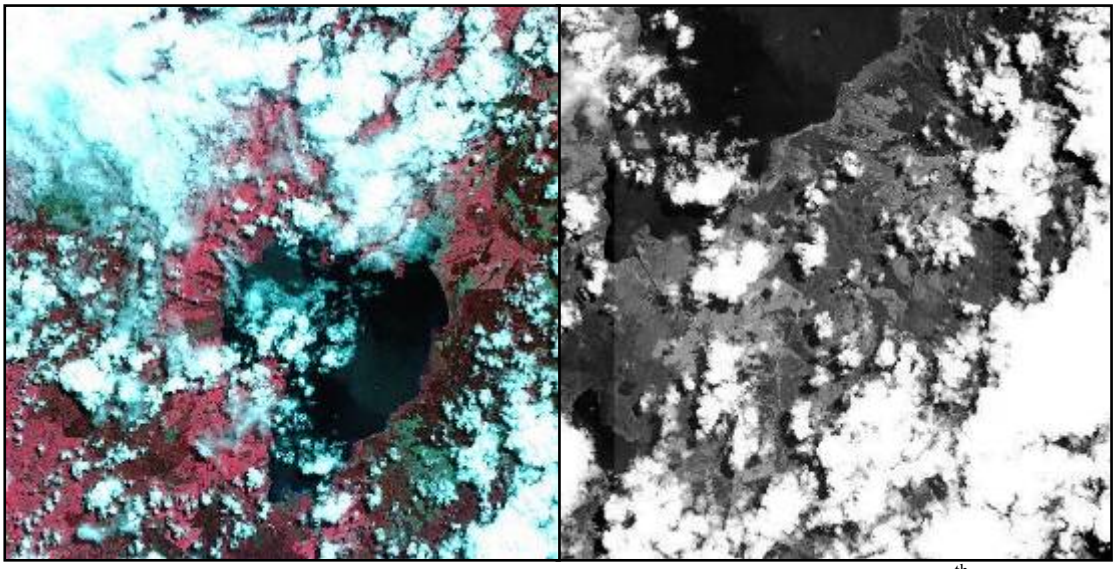

Figure 13: ALOS satellite's AVNIR-2 and PRISM data over Lake Taupo, acquired on 30th Nov 2006.

Figure 14: QuickBird satellite scene captured on 22nd March 2007, showing the Area of Interest (AOI)

3.4. Ground based RS data validation / ancillary data

The lack of a sufficient number of ground truth sites is often a limiting factor in the classification of satellite images as well as its proper validation. Field visits to correlate physically estimated biomass with pixel reflectance are time consuming and often limited due to accessibility. Lieng et al. (2003) suggest that capturing detailed information of the landscape from an airplane is an alternative approach towards collecting ground truth data. Therefore, QuickBird data from the same time of year has been identified and purchased. If the geographic registration issue among different datasets is addressed then use of high resolution satellite or aerial images can significantly help in identifying the end-members for image classification. High spatial resolution data can also quantify the mixing percentage of different end members in the corresponding pixel of low spatial resolution datasets.

Malthus and George (1997) suggest that part of the problem with mapping aquatic plants using digital techniques is due to insufficient information about the *in-situ* spectral reflectance properties of the macrophytes. Development of a spectral library for different macrophytes under different water quality parameters will help to determine the most appropriate bands for identification and determination of biophysical parameters of rooted but emergent as well as submerged aquatic plant species. Thus this study requires establishing an *in-situ* spectral reflectance library for different end members so that this information can be used for better classification of the RS data.

3.5. Selection of image processing techniques

Digital image processing involves the manipulation and interpretation of digital images with the aid of a computer. Digital image processing is an extremely broad subject which includes a range of different operations performed on it. Lillesand et al. (2004) have put together typical computer assisted operations in the following groups:

i) Image rectification and restoration, sometimes referred to as pre-processing,
ii) Image enhancement,
iii) Image classification,
iv) Data merging and GIS integration,
v) Hyperspectral image analysis,
vi) Biophysical modelling, and
vii) Image transmission and compression.

Most of these operations are performed on datasets that are converted from mere pixel reflectance values into meaningful information. Our prime concern is very much associated with the discussion on biophysical modelling and image classification.

Biophysical modelling refers to the process of quantitatively relating remotely sensed data to biophysical features or phenomena on the earth's surface. In our case, it is the quantitative measure of chlorophyll *a* or its biomass prediction with or without using ground based observations. Three basic approaches are employed in the processing of data. The first one deals with the *empirical modelling* in which correlations are established between radiometric reflectance of RS and ground data. In the *physical modelling*, all the physical parameters of any RS data are mathematically accounted for. The physical parameters that can influence radiometric values of RS data include

earth-sun distance, solar elevation, seasonal and atmospheric effects and viewing geometry. The third approach to biophysical modelling is to employ a combination of physical and empirical models e.g. converting DN values to absolute radiance prior to relating these values to a ground based dataset (Lillesand et al., 2004). This biophysical modelling is a standard procedure to determine chlorophyll *a* and suspended sediment concentration in open water bodies. Literature reviewed and discussed in the previous chapter show that limnetic remote sensing has mostly used empirical (like bands ratios) and biophysical models to determine different water quality parameters. However, some literature used advanced image classification techniques like linear mixture modelling and neural network classification to achieve their objectives (Rogge et al., 2007, Sudheer et al., 2006, Tyler et al., 2006).

The overall objective of image classification procedures is to automatically categorise all the image pixels into themes or classes (Lillesand et al., 2004). A conventional supervised per-pixel or hard classifier assigns each pixel a particular class considering its similarities based on the representative spectral values of the sample data, generally referred to as training fields (Lillesand et al., 2004; Verbyla, 1995). Eventually the mixed-pixels or mixels are assigned to the most similar class which results in decreased classification accuracy; it is thus desirable to unmix the spectral response of the mixed pixels (Shanmugam et al., 2006). A common way to unmix this is through Linear Spectral Mixture Modelling (LSMM) which is suitable for handling the spectral mixture problem, mainly because: (i) it does not require extensive training data, (ii) it produces a set of maps, one for each class type concerned, and (iii) it was extensively applied to extract the abundance of various components within the mixed pixels of satellite data of similar environments. The goal of linear spectral mixture modelling is to estimate the fractional cover of each major landscape unit of interest within image pixels. The required inputs to LSMM are end-member reflectance. The output is a fraction image, with coefficients lying between 0 and 1 and summing to 1, for each end-member along with an image containing an error of fit.

The principal assumption of LSMM is that the measured reflectance of a pixel is the linear sum of the reflectance of the mixture components that make up that pixel. In order for the LSMM to be applied, the reflectance of that pixel is assumed to be formed as the sum of the reflectance of the end-member types weighted by their proportions (Shanmugam et al., 2006). The limitation with this approach is that the number of end members should always be one less than the number of spectral bands available in the image. This technique is thus limited to counting a large and complex number of combinations of materials or end-members that can occur within a single pixel (Boudreau et al., 1996). For example, if using this technique on ALOS AVNIR-2 data, it will accommodate only 3 end members.

IMAGINE *Subpixel Classifier* is another supervised classification tool that detects and reports whole and subpixel occurrences of a specific Material of Interest in multispectral imagery. IMAGINE Subpixel Classifier derives a signature for a specific material, groups all pixels in an image as either containing the material or not, and classifies all pixels that do contain the material into classes based on how much of the material they contain. Subpixel Classifier differs from both traditional classifiers and spectral mixing models by allowing the user to develop a highly specific, whole or subpixel spectral signature for a particular material of interest (MOI). This not only allows for the development of 'purer' signatures, but using an innovative background

removal technique that removes all dissimilar materials from each pixel results in a higher degree of discrimination sensitivity, and thus a classification of greater accuracy. The output is an overlay image indicating pixels containing the MOI in either two (0.4 increments), four (0.2 increments), or eight (0.1 increments) classes, greater than 20 percent. The subpixel classification procedure is facilitated by a number of automated processes, including environmental correction that makes subpixel material detection easier, more accurate, and less time-consuming (Flanagan and Civco, 2001). The subpixel process does not provide information on where the material of interest occurs within the pixel. It does provide important information on the relative proportion of the material of interest found within a pixel (Huguenin et al., 1997).

Huguenin et al. (1997) define subpixel processing as the search for specific materials of interest from within a pixel's mixed multispectral image digital number spectrum. Another advantage with subpixel classifier is its environmental correction of the studied multispectral data offering freedom to transfer end-members selection over space and time. Using this tool, even high resolution satellite data captured in multiple scenes can be processed with ease.

3.6. Discussion

Satellite remote sensing and aerial imaging, both have limitations in their own spheres of operation. The following characteristics can be judged as tradeoffs for selecting among available (aerial or space borne) options in order to monitor heterogeneous environments over a reasonably large area.

3.6.1. Sensor capabilities

In terms of data quality parameters, satellite data have more disadvantages than aerial photography. Once a satellite is fabricated and launched, the choices for changing the sensor characteristics and users are bound to live with its inherent spatial, spectral and radiometric resolutions. Although side viewing technology has the ability to revisit more quickly than its nadir flyover, but it usually introduces geometric distortion and reduced spatial resolution which impacts on overall data quality. In aerial imaging, users have more control to acquire data according to their requirements. A longer focal length lens can substantially improve ground sample distance. Moreover, it is possible to choose aerial sensors according to need.

3.6.2. Efficiency

Satellite RS data is effective and efficient in its ability to scan the earth quickly due to its larger swathe and orbiting position. Landsat takes only 15 days to completely scan all parts of the globe. This is very efficient if it is compared with aerial reconnaissance. However, if compared with other satellites, 15 days is still a lot. In newly launched satellites, special emphasis has been given to increase their spatial extent. As a result the newly launched DMC (Disaster Monitoring Consortium) series satellites offer 32m spatial resolution data with a 600km swathe. There are four satellites capable of capturing data in the similar mode and these can scan the entire globe in 2-4 data time at a resolution on par with Landsat. Similarly, IRS-6P

(ResourceSat) offers AWiFS data at 56m resolution over a 740km wide swathe, and thus it alone can cover the entire globe in 4-5 days.

3.6.3. Cost of data

Although satellites are expensive to build, launch and maintain, a recent drive towards lower cost, more frequently launched, smaller satellites has brought in low cost data. However, satellite images are cost effective only if the scale of the study is national to global. For a smaller region, digital aerial images are quite cheap and quickly available after capture. Conventional photographic film cameras require additional steps to process and then scan to bring in to the system for further processing so there can be little doubt that digital imaging is far more efficient than conventional photography. The cost of airborne data on a unit image basis is probably highest. It also depends on the type of aerial platform. Low flying ultra-light aircraft are cheaper to operate but take more time to capture data. High altitude aerial photography is expensive and requires precise sensors to capture the data.

Davis (2002) has provided an estimate of different aerial photography datasets for the Colorado River. This cost varied from scanned photographic CIR and digital CCD based CIR data (both costing $225/line km) to multispectral scanner (using Aerial Thematic Mapper) data (costing $620/line km).

3.6.4. Operational limitations

In terms of other physical quality parameters, satellite images are better than aerial data. For example, satellites fly in a very stable orbit so distortions in data geometry are negligible. Recent advancements in the field of digital aerial photography have minimised these limitations such as a combination of GPS and INS (inertial navigation system) record the flight altitude and attitude and provides the ability to quickly process the data.

3.6.5. Ease of data acquisition and analyses

The greater swathe width and removal of data artefacts of satellite sensors makes for more consistent data for analyses including mosaicing of data scenes. These sensors also tend to remain more constant over time to facilitate time series analyses. Relatively larger areas which tend to fall in tens to hundreds of the small scenes of high-resolution satellite or airborne sensors make data acquisition and its processing more time consuming.

3.6.6. Frequency of data observation

Observations with aircraft are possible virtually any time of day or day of the week, depending upon weather and budgetary constraints. This freedom has long attracted scientists and end users, particularly when there are important timing considerations to take into account. An airborne sensor can also be flown at several altitudes within reason to obtain a set of observations at different spatial resolutions (Peterson et al., 2003).

3.6.7. Estimated cost of RS data

The Waikato region is poorly captured in terms of RS data. For the satellite based data acquisition, unsuitable meteorological conditions have contributed to a paucity of cloud free images. Aerial photography has been conducted with inherent low spectral reflectance in the past, e.g. WRAPS 1993 and 2002 datasets, and this limits its use in remote sensing.

Table 6: Estimated cost to study large lakes and rivers in the Waikato region

Satellite	Sensor	No. of images needed to cover the entire region	Unit cost ($NZ)	Estimated cost ($NZ)	Ease of Processing (1-5)*	Accuracy
Landsat	TM	2	1350	2700	1	☹
ResourceSat	AWiFS	1	2700	2700	1	☹
Spot-5	XS	15	5800	87000	2	😐
	PAN		5800	87000		
ALOS	AVNIR-2	10	330+	3300	2	☺
	PRISM	40		13200		
QuickBird	Bundled	75	5000	375000	4	☺
Terra	ASTER	15	135	2025	2	☹
EO-1	ALI	50	525	26250	3	😐
	Hyperion	200	525	105000	4	☹
Spot-4	XS	15	4250	63750	2	😐
	PAN	15	4250	63750	2	
CASI-2	Hyperspectral	Multiple	?	?	4	☺
Customised multispectral digital camera	Minimum 4 no of cameras	Multiple	~5000	20000	5	☺
	A gyro-mount (optional)		~4500	4500		
	Flying hours	50	150	7500		

* 1 = easy; 5 = hard

\+ Indicating non-commercial price; commercial cost is 3 times more

☺ Meets requirement

😐 Satisfactory but not a preferred choice

☹ Does not meet requirement

It should be noted that the estimated cost for each satellite in Table 5 is for its archived data. Cost for new acquisition is usually higher than the archived image. It is evident that cost of high-resolution images (e.g. QuickBird) is quite high if capturing the entire Waikato region at once. The *All of Government* initiative has lessened its cost to a feasible level, thus it offers perhaps the best choice in terms of spatial resolution to map aquatic habitat. Due to its narrow swathe, it may require more than one season to cover the entire region for one time data acquisition. ALOS is also quite reasonable in its price, however it carries limited archived data over the Waikato region. It offers a potential data source to map the aquatic vegetation within the Waikato region. In the case of acquiring new ALOS images, one may need to pay the full fee i.e. three times the cost of its non-commercial data cost.

Chapter 4

Summary and Recommendations for Further Work

The review of satellite sensors available in NZ for aquatic mapping has identified three data options, which have been purchased for a case study area (Tongariro river delta). These data options are Landsat-5 (30m resolution), ALOS (2.5m), and QuickBird-2 (0.6m). There is no one perfect option available as each option is a compromise between spatial and spectral resolution, and cost. The Quickbird-2 option may be feasible if the "Kiwimage" initiative to purchase Quickbird-2 data for all of NZ eventuates. Developing tools and classification techniques using Quickbird-2 could potentially be very useful to Environment Waikato for mapping aquatic environments if "Kiwimage" eventuates. ALOS also provides a cost effective option, especially if the non-commercial pricing available to the Waikato University is used. The main problem with ALOS, being a recent satellite, is the limited archive of images for Waikato, as this is a recent satellite. The availability for the Waikato region, which is often cloudy, may cause problems. Landsat-5 offers an extensive archive and relatively cheap acquisition with good spectral resolution but compromised spatial resolution. The combination of Landsat 5 and ALOS may produce a feasible option for regular mapping of aquatic environments. In addition to satellite images there is also existing WRAPS aerial images with 1m spatial resolution. These images could possibly be used in combination with satellite images.

To obtain the most from these data sets, field based (in-situ) data needs to be collected so that accurate spectral signatures of different vegetation can be obtained and used to train classification algorithms.

We recommend the following work in relation to the data sets discussed above:

1. Compare different classification algorithms such as supervised and sub pixel classification using the case study area and the ALOS, Landsat-5, Quickbird-2, and WRAPS images.

2. Combine (fuse) ALOS, Landsat-5, and WRAPS images to increase the spectral and spatial resolutions and assess its performance with a range of classification techniques.

3. Collect *in-situ* spectral reflectance data for predominant species and species assemblages (of terrestrial, emergent and submerged vegetation) at different water quality parameters for the case study area. This will improve sub pixel classification accuracy and will also help in identifying suitable spectral bands.

An alternative or complimentary approach could be to investigate the use of a digital camera for taking vertical aerial images. This would begin with a standard SLR camera with a set of different band-pass filters, which can capture different band

widths, including non visual infra-red bands up to 1μm. This camera would need to be a digital monochrome (black and white) camera, which can be purchased at the same costs as a colour camera. The filters cost $200 each and 6-8 different filters are needed. Images would be captured using a light aeroplane flying above the minimum ground elevation of 500m. These images would then be manually geo-referenced in a GIS. This system may have considerable potential for regular and cost effective mapping of aquatic environments. It may also have many other applications for monitoring water quality, fish counting, and land use change. If this trial with a cheap camera is successful, then the development of a purpose-built camera and mounting equipment, which range in costs from $10,000 to $20,000 dollars, should be considered to ensure long-term monitoring.

Acknowledgements:

We thank Kevin Collier and Keri Neilson, Environment Waikato (EW), for helping to devise the study objectives, and for their critical input. Funding was provided by EW and a FRST OBI contract UOWX050. Mathew Allan gave useful comments on the application of remote sensing to monitor water quality for large water bodies. We appreciate his efforts and support.

References:

Apan, A.A., Raine, S.R. and Paterson, M.S., 2002. Mapping and analysis of changes in the riparian landscape structure of the Lockyer Valley catchment, Queensland, Australia. Landscape and Urban Planning, 59(1): 43-57.

Avery, T.E., 1968. Interpretation of Aerial Photographs. Burgess Publishing Co., Minneapolis, 392 pp.

Baban, S.M.J., 1993. Detecting water quality parameters in the Norfolk Broads, U.K., using Landsat imagery. International Journal of Remote Sensing, 14(7): 1247 – 1267.

Bajjouk, T., Populus, J. and Guillaumont, B., 1998. Quantification of Subpixel Cover Fractions Using Principal Component Analysis and a Linear Programming Method: Application to the Coastal Zone of Roscoff (France). Remote Sensing of Environment, 64(2): 153-165.

Barnes, G., 2002. Water quality trends in selected shallow lakes in the Waikato region: 1995-2001. Technical Report No. 2002/11, Environment Waikato, Hamilton, NZ.

Becker, B.L., Lusch, D.P. and Qi, J., 2005. Identifying optimal spectral bands from in situ measurements of Great Lakes coastal wetlands using second-derivative analysis. Remote Sensing of Environment, 97(2): 238-248.

Becker, B.L., Lusch, D.P. and Qi, J., 2007. A classification-based assessment of the optimal spectral and spatial resolutions for Great Lakes coastal wetland imagery. Remote Sensing of Environment, 108(1): 111-120.

Belluco, E. et al., 2006. Mapping salt-marsh vegetation by multispectral and hyperspectral remote sensing. Remote Sensing of Environment, 105(1): 54-67.

Bierwirth, P.N., Lee, T.J. and Burne, R.V., 1993. Shallow Sea-Floor Reflectance and Water Depth Derived by Unmixing Multispectral Imagery. Photogrammetric Engineering and Remote Sensing, 59(3): 331-338.

Booth, D.T., Cox, S.E. and Berryman, R.D., 2006. Precision measurements from very-large scale aerial digital imagery. Environmental Monitoring and Assessment, 112(1-3): 293-307.

Booth, D.T., Cox, S.E. and Simonds, G., 2007. Riparian monitoring using 2-cm GSD aerial photography. Ecological Indicators, 7(3): 636-648.

Boudreau, E.R., Huguenin, R.L. and Karaska, M.A., 1996. Nonparametric classification of subpixel materials in multispectral imagery. In: A.E. Iverson (Editor), Algorithms for Multispectral and Hyperspectral Imagery II. SPIE, Bellingham, WA, pp. 31-39.

Bowen, Z.H. and Waltermire, R.G., 2002. Evaluation of light detection and ranging (LIDAR) for measuring river corridor topography. Journal of the American Water Resources Association, 38(1): 33-41.

Brönmark, C. and Hansson, L.A., 2005. The Biology of Lakes and Ponds. Oxford University Press, Oxford, 285 pp.

Brown, A.L., 1987. Freshwater Ecology. Heinimann Educational Books, London, 163 pp.

Bukata, R.P., Jerome, J.H., Kondratyev, K.Y., Pozdnyakov, D.V. and Kotykhov, A.A., 1997. Modelling the radiometric color of inland waters: Implications to a) remote sensing and b) limnological color scales. Journal of Great Lakes Research, 23(3): 254-269.

Caloz, R. and Collet, C., 1997. Geographic information systems (GIS) and remote sensing in aquatic botany: methodological aspects. Aquatic Botany, 58(3-4): 209-228.

Collier, K.J. et al., 1995. Managing Riparian Zones: A contribution to protecting New Zealand's rivers and streams, Vol 1: Concepts. Department of Conservation, Wellington, New Zealand, 56 pp.

Comer, R.P., Kinn, G., Light, D. and Mondello, C., 1998. Talking digital. Photogrammetric Engineering and Remote Sensing, 64(12): 1139-1142.

Congalton, R.G., Birch, K., Jones, R. and Schriever, J., 2002. Evaluating remotely sensed techniques for mapping riparian vegetation. Computers and Electronics in Agriculture, 37(1-3): 113-126.

Davies, S.W. and Merton, R.N., 2007. Bathymetric & benthic investigation of coastal lake environments using multi-angle CHRIS/proba hyperspectral data, Proceedings of the Spatial Science Institute Biennial International Conference (SSC 2007), Hobart, Tasmania, Australia, 14-18 May 2007, pp. 937-949 (non refereed paper).

Davis, P.A., 2002. Evaluation of airborne thermal-infrared image data for monitoring aquatic habitats and cultural resources within the Grand Canyon. Open File Report 02-367, USGS, Flagstaff, AZ.

Davis, P.A., Staid, M.I., Plescia, J.B. and Johnson, J.R., 2002. Evaluation of airborne image data for mapping riparian vegetation within the Grand Canyon. Open File Report 02-470, USGS, Flagstaff, AZ.

Dekker, A.G., Vos, R.J. and Peters, S.W.M., 2002. Analytical algorithms for lake water TSM estimation for retrospective analyses of TM and SPOT sensor data. International Journal of Remote Sensing, 23(1): 15-35.

Edwards, T., Clayton, J. and Winton, M.d., 2007. The condition of 41 lakes in the Waikato region using LakeSPI. NIWA Client Report HAM2007-108, National Institute of Water and Atmospheric Research Ltd., Hamilton, New Zealand.

Edwards, T., Clayton, J. and Winton, M.d., 2005. The conditions of lakes in the Waikato region using LakeSPI. Technical Report No. 2006/13, Environment Waikato, Hamilton, New Zealand.

Flanagan, M. and Civco, D.L., 2001. IMAGINE Subpixel Classifier Version 8.4. Photogrammetric Engineering & Remote Sensing, 67(1): 23 – 28.

Flotemersch, J.E., Stribling, J.B. and Paul, M.J., 2006. Concepts and Approaches for the Bioassessment of Non-wadeable Streams and Rivers, US Environmental Protection Agency, Cincinnati, Ohio.

Gattuso, J.P., Frankignoulle, M. and Wollast, R., 1998. Carbon and carbonate metabolism in coastal aquatic ecosystems. Annual Review of Ecology and Systematics, 29: 405-434.

Gilvear, D., Hunter, P. and Higgins, T., 2007. An experimental approach to the measurement of the effects of water depth and substrate on optical and near infra-red reflectance: a field-based assessment of the feasibility of mapping submerged instream habitat. International Journal of Remote Sensing, 28(10): 2241 – 2256.

Goetz, S.J., 2006. Remote sensing of riparian buffers: Past progress and future prospects. Journal of the American Water Resources Association, 42(1): 133-143.

Goetz, S.J., Wright, R.K., Smith, A.J., Zinecker, E. and Schaub, E., 2003. IKONOS imagery for resource management: Tree cover, impervious surfaces, and

riparian buffer analyses in the mid-Atlantic region. Remote Sensing of Environment, 88(1-2): 195-208.

Graham, R.W. and Mills, J.P., 2000. Small format digital cameras for aerial survey: Where are we now? Photogrammetric Record, 16(96): 905-909.

Hebert, P., Sagarin, R., 2007. "Macrophytes" In: Encyclopedia of Earth. Eds. Cleveland, C. J. Environmental Information Coalition, National Council for Science and the Environment, Washington D.C. [Published April 2, 2007; Retrieved September 10, 2007].<http://www.eoearth.org/article/Macrophytes>

Heipke, C., Jacobsen, K. and Mills, J., 2006. Theme issue: Digital aerial cameras. ISPRS Journal of Photogrammetry and Remote Sensing, 60(6): 361-362.

Held, A., Ticehurst, C., Lymburner, L. and Williams, N., 2003. High resolution mapping of tropical mangrove ecosystems using hyperspectral and radar remote sensing. International Journal of Remote Sensing, 24(13): 2739 – 2759.

Honkavaara, E. et al., 2006. Geometric test field calibration of digital photogrammetric sensors. ISPRS Journal of Photogrammetry and Remote Sensing, 60(6): 387-399.

Huguenin, R.L., Karaska, M.A., VanBlaricom, D. and Jensen, J.R., 1997. Subpixel classification of bald cypress and tupelo gum trees in thematic mapper imagery. Photogrammetric Engineering and Remote Sensing, 63(6): 717-725.

Jensen, J.R. et al., 1986. Remote sensing inland wetlands: A multispectral approach. Photogrammetric Engineering, 52(1): 87−100.

Johansen, K. and Phinn, S., 2006a. Linking riparian vegetation spatial structure in Australian tropical savannas to ecosystem health indicators: semi-variogram analysis of high spatial resolution satellite imagery. Canadian Journal of Remote Sensing, 32(3): 228-243.

Johansen, K. and Phinn, S., 2006b. Mapping structural parameters and species composition of riparian vegetation using IKONOS and acroph ETM plus data in Australian tropical savannahs. Photogrammetric Engineering and Remote Sensing, 72(1): 71-80.

Johansen, K., Phinn, S., Dixon, I., Douglas, M. and Lowry, J., 2007. Comparison of image and rapid field assessments of riparian zone condition in Australian tropical savannas. Forest Ecology and Management, 240(1-3): 42-60.

Joyce, K.E., 2004. A method of mapping live coral cover using remote sensing, University of Queensland, Brisbane, 137 pp.

Kloiber, S.N., Brezonik, P.L., Olmanson, L.G. and Bauer, M.E., 2002. A procedure for regional lake water clarity assessment using Landsat multispectral data. Remote Sensing of Environment, 82(1): 38-47.

Konecny, G., 1994. New trends in technology, and their applications: photogrammetry and remote sensing from analog to digital, Thirteenth United Nations Regional Cartographic Conference for Asia and the Pacific, Beijing, 9-15 May 1994.

Kutser, T., Metsamaa, L., Strombeck, N. and Vahtmae, E., 2006a. Monitoring cyanobacterial blooms by satellite remote sensing. Estuarine, Coastal and Shelf Science, 67(1-2): 303-312.

Kutser, T., Miller, I. and Jupp, D.L.B., 2006b. Mapping coral reef benthic substrates using hyperspectral space-borne images and spectral libraries. Estuarine, Coastal and Shelf Science, 70(3): 449-460.

Lieng, E., Slaymaker, D. and Kastdalen, L., 2003. Use of airborne small-frame digital cameras as tools for collecting ground truth. Hedmark University College, Koppang, Norway, pp. 1-4.

Light, D.L., 1996. Film cameras or digital sensors? The challenge ahead for aerial imaging. Photogrammetric Engineering and Remote Sensing, 62(3): 285-291.

Lillesand, T.M., Kiefer, R.W. and Chipman, J.W., 2004. Remote sensing and image interpretation. , 5th ed. John Wiley &. Sons Inc, New York, NY.

Lonard, R.I. et al., 2000. Evaluation of color-infrared photography for distinguishing annual changes in riparian forest vegetation of the lower Rio Grande in Texas. Forest Ecology and Management, 128(1-2): 75-81.

LPS, 2006. Stereo Analyst User's Guide. Leica Geosystems Geospatial Imaging, LLC, Norcross, GA, USA.

Maheu-Giroux, M. and Blois, S.d., 2005. Mapping the invasive species Phragmites australis in linear wetland corridors. Aquatic Botany, 83(4): 310-320.

Malthus, T.J. and George, D.G., 1997. Airborne remote sensing of macrophytes in Cefni Reservoir, Anglesey, UK. Aquatic Botany, 58(3-4): 317-332.

Malthus, T.J. and Karpouzli, E., 2003. Integrating field and high spatial resolution satellite-based methods for monitoring shallow submersed aquatic habitats in the Sound of Eriskay, Scotland, UK. International Journal of Remote Sensing, 24(13): 2585 – 2593.

Malthus, T.J. and Mumby, P.J., 2003. Remote sensing of the coastal zone: an overview and priorities for future research. International Journal of Remote Sensing, 24(13): 2805 – 2815.

Marshall, T.R. and Lee, P.F., 1994. Mapping Aquatic Macrophytes through Digital Image-Analysis of Aerial Photographs – an Assessment. Journal of Aquatic Plant Management, 32: 61-66.

Mathews, B., 1998. An ultra high resolution, electro-optical framing camera for reconnaissance and other applications using a 9216 by 9216 pixel, wafer scale, focal plane array. In: W.G. Fishell, A.A. Andraitis, M.S. Fagan, J.D. Greer and M.C. Norton (Editors), Airborne Reconnaissance Xxii. Proceedings of the Society of Photo-Optical Instrumentation Engineers (Spie), pp. 144-154.

Mayo, M., Gitelson, A., Yacobi, Y.Z. and Benavraham, Z., 1995. Chlorophyll Distribution in Lake Kinneret Determined from Landsat Thematic Mapper Data. International Journal of Remote Sensing, 16(1): 175-182.

Mount, R.E., 2006. Small format digital aerial photography for mapping and monitoring seagrass habitats in shallow temperate marine waters, University of Tasmania, Hobart, 185 pp.

Muller, E., 1997. Mapping riparian vegetation along rivers: old concepts and new methods. Aquatic Botany, 58(3-4): 411-437.

Mumby, P.J. and Edwards, A.J., 2002. Mapping marine environments with IKONOS imagery: enhanced spatial resolution can deliver greater thematic accuracy. Remote Sensing of Environment, 82(2-3): 248-257.

Nagler, P., Glenn, E.P., Hursh, K., Curtis, C. and Huete, A., 2005. Vegetation mapping for change detection on an arid-zone river. Environmental Monitoring and Assessment, 109(1-3): 255-274.

Nagler, P.L., Glenn, E.P. and Huete, A.R., 2001. Assessment of spectral vegetation indices for riparian vegetation in the Colorado River delta, Mexico. Journal of Arid Environments, 49(1): 91-110.

Narumalani, S., Zhou, Y.C. and Jensen, J.R., 1997. Application of remote sensing and geographic information systems to the delineation and analysis of riparian buffer zones. Aquatic Botany, 58(3-4): 393-409.

Nelson, S.A.C., Cheruvelil, K.S. and Soranno, P.A., 2006. Satellite remote sensing of freshwater macrophytes and the influence of water clarity. Aquatic Botany, 85(4): 289-298.

NIWA-Science, 2007. Monthly national climate summaries. National Climate Centre, NIWA Science.

OEPC, 1994. The Impact of Federal Programs on Wetlands – Volume II: The Everglades, Coastal Louisiana, Galveston Bay, Puerto Rico, California's Central Valley, Western Riparian Areas, Southeastern and Western Alaska, The Delmarva Peninsula, North Carolina, Northeastern New Jersey, Michigan, and Nebraska. Office of Environment Policy and Compliance, US Department of the Interior, Washington D.C.

Oestlund, C., Flink, P., Stroembeck, N., Pierson, D. and Lindell, T., 2001. Mapping of the water quality of Lake Erken, Sweden, from Imaging Spectrometry and Landsat Thematic Mapper. The Science of the Total Environment, 268: 139-154.

Peterson, D.L. et al., 2003. Platform options of free-flying satellites, UAVs or the International Space Station for remote sensing assessment of the littoral zone. International Journal of Remote Sensing, 24(13): 2785-2804.

Pulliainen, J. et al., 2001. A semi-operative approach to lake water quality retrieval from remote sensing data. Science of the Total Environment, 268(1-3): 79-93.

Raitala, J., Jantunen, H. and Lampinen, J., 1985. Application of Landsat satellite data for mapping aquatic areas in north-eastern Finland. Aquatic Botony, 21: 285-294.

Reinart, A. and Kutser, T., 2006. Comparison of different satellite sensors in detecting cyanobacterial bloom events in the Baltic Sea. Remote Sensing of Environment, 102(1-2): 74-85.

Rogge, D.M. et al., 2007. Integration of spatial-spectral information for the improved extraction of endmembers. Remote Sensing of Environment, 110(3): 287-303.

Sabol, B.M., Melton, R.E., Chamberlain, R., Doering, P. and Haunert, K., 2002. Evaluation of a digital echo sounder system for detection of submersed aquatic vegetation. Estuaries, 25(1): 133-141.

Schulz, M., Rinke, K. and Kohler, J., 2003. A combined approach of photogrammetrical methods and field studies to determine nutrient retention by submersed macrophytes in running waters. Aquatic Botany, 76(1): 17-29.

Schwarz, A.-M., Howard-Williams, C. and Clayton, J., 2000. Analysis of relationships between maximum depth limits of aquatic plants and underwater light in 63 New Zealand lakes. New Zealand Journal of Marine and Freshwater Research, 34: 157-174.

Senay, G.B., Shafique, N.A., Autrey, B.C., Fulk, F. and Cormier, S.M., 2001. The selection of narrow wavebands for optimizing water quality monitoring on the Great Miami River, Ohio using hyperspectral remote sensor data. Journal of Spatial Hydrology, 1(1): 1-22.

Shanmugam, P., Ahn, Y.-H. and Sanjeevi, S., 2006. A comparison of the classification of wetland characteristics by linear spectral mixture modelling and traditional hard classifiers on multispectral remotely sensed imagery in southern India. Ecological Modelling, 194(4): 379-394.

Sotheran, I.S., FosterSmith, R.L. and Davies, J., 1997. Mapping of marine benthic habitats using image processing techniques within a raster-based geographic information system. Estuarine Coastal and Shelf Science, 44: 25-31.

Sudheer, K.P., Chaubey, I. and Garg, V., 2006. Lake water quality assessment from Landsat Thematic Mapper data using neural network: An approach to optimal band combination selection Journal of the American Water Resources Association, 42(6): 1683 – 1695.

Tyler, A.N., Svab, E., Preston, T., Presing, M. and Kovacs, W.A., 2006. Remote sensing of the water quality of shallow lakes: A mixture modelling approach to quantifying phytoplankton in water characterized by high-suspended sediment. International Journal of Remote Sensing, 27(8): 1521 – 1537.

Valley, R.D., Drake, M.T. and Anderson, C.S., 2005. Evaluation of alternative interpolation techniques for the mapping of remotely-sensed submersed vegetation abundance. Aquatic Botany, 81(1): 13-25.

Valta-Hulkkonen, K., Pellikka, P., Tanskanen, H., Ustinov, A. and Sandman, O., 2003. Digital false colour aerial photographs for discrimination of aquatic macrophytes species. Aquatic Botany, 75(1): 71-88.

Vant, B. and Smith, P., 2004. Trends in river water quality in the Waikato Region, 1987-2002. Technical Report No. 2004/02, Environment Waikato, Hamilton, NZ.

Vant, W.N., Davies-Colley, R.J., Clayton, J.S. and Coffey, B.T., 1986. Macrophyte depth limits in North Island (New Zealand) lakes of differing clarity. Hydrobiologia, 137: 55-60.

Verbyla, D.L., 1995. Satellite remote sensing of natural resources. Mapping sciences series. Lewis Publishers, Boca Raton, FL.

Vis, C., Hudon, C. and Carignan, R., 2003. An evaluation of approaches used to determine the distribution and biomass of emergent and submerged aquatic macrophytes over large spatial scales. Aquatic Botany, 77(3): 187-201.

Weber, R.M. and Dunno, G.A., 2001. Riparian vegetation mapping and image processing techniques, Hopi Indian Reservation, Arizona. Photogrammetric Engineering and Remote Sensing, 67(2): 179-186.

White, W.H., Harborne, A.R., Sotheran, I.S., Walton, R. and Foster-Smith, R.L., 2003. Using an Acoustic Ground Discrimination System to map coral reef benthic classes. International Journal of Remote Sensing, 24(13): 2641-2660.

Whited, D., Stanford, J.A. and Kimball, J.S., 2002. Application of airborne multispectral digital imagery to quantify riverine habitats at different base flows. River Research and Applications, 18(6): 583-594.

Wilding, T.A., Sayer, M.D.J. and Provost, P.G., 2003. Factors affecting the performance of the acoustic ground discrimination system RoxAnn ™. Ices Journal of Marine Science, 60(6): 1373-1380.

Wolter, P.T., Johnston, C.A. and Niemi, G.J., 2005. Mapping submergent aquatic vegetation in the US Great Lakes using Quickbird satellite data. International Journal of Remote Sensing, 26(23): 5255-5274.

Wright, A., Marcus, W.A. and Aspinall, R., 2000. Evaluation of multispectral, fine scale digital imagery as a tool for mapping stream morphology. Geomorphology, 33(1-2): 107-120.

Yang, X., 2007. Integrated use of remote sensing and geographic information systems in riparian vegetation delineation and mapping. International Journal of Remote Sensing, 28(1-2): 353-370.

Zilioli, E. and Brivio, P.A., 1997. The satellite derived optical information for the comparative assessment of lacustrine water quality. Science of the Total Environment, 196(3): 229-245.

Appendix A: Review of Remote Sensing Platforms and Digital Sensors

A.1. Introduction to remote sensing

Remote sensing is myopically termed as a process of acquiring data about an object or area from a distance. Data acquisition heavily depends upon source of energy (usually the sun) to strike an object or an area that is under investigation. Three possible interactions can then occur simultaneously. The energy can be reflected, transmitted or be absorbed, which is based on the physical properties of the object or area. A sensor at a distance records this information based on the net energy reflected from the object. A sensor can carry its own source of electromagnetic energy (EME), which is referred to as *active remote sensing*. Sun is a typical source of electromagnetic energy to the Earth. Capturing information of an object using solar energy is termed as *passive remote sensing*. The data captured is always presented as an image and data processing involves analysing this image. There are numerous platforms that are used to acquire remotely sensed data. Based on their altitude, these platforms are classified into two broad categories i.e. airborne and space borne remote sensing.

A.2. Aerial photography and photogrammetry

Aerial photography is the most common and versatile form of remote sensing which started soon after the invention of photography. It used different platforms during its evolution, ranging from hot air balloons to kites. The aeroplane which had been invented in 1903 was not used for aerial photography until 1908. Once started, aerial photography received heightened attention in the interest of military reconnaissance during World War I. Over the period of time, information extraction from the aerial images became more established discipline, called *photogrammetry*.

Photogrammetry is the "art, science and technology of obtaining reliable information about physical objects and the environment through the process of recording, measuring and interpreting photographic images and patterns of electromagnetic radiant imagery and other phenomena" (LPS, 2006). The traditional, and largest, application of photogrammetry is to extract topographic and planimetric information (for example, topographic maps) from aerial images. However, photogrammetric techniques have also been applied to process satellite images and close-range images to acquire topographic or non-topographic information of photographed objects. Topographic information includes spot height information, contour lines, and elevation data. Planimetric information includes the geographic location of buildings, roads, rivers, etc.

Photogrammetry was invented in 1851 by Laussedat, and has continued to develop over the last 150 years. Over time, the development of photogrammetry has passed through the phases of plane table photogrammetry, analogue photogrammetry, analytical photogrammetry, and has now entered the phase of digital photogrammetry (Konecny, 1994).

Plane table photogrammetry was established prior to the invention of the airplane, when photographs taken on the ground were used to extract the relationship between

objects using geometric principles. Analogue photogrammetry became established in its true essence with the use of stereo measurement equipment in 1901. Optical or mechanical instruments, such as the analogue plotter, were used to reconstruct 3D geometry from two overlapping photographs. This phase resulted in regional to national scale production of topographic maps. In analytical photogrammetry, the computer technology replaced some expensive optical and mechanical components. The resulting devices were analogue/digital hybrids. This phase resulted in development of topographic maps along with other digital products, such as digital maps and digital elevation models (DEMs) (LPS, 2006). This technique is still widely used in most parts of the world including New Zealand.

Recent technological advances in data capture and its computation have automated many photogrammetric tasks. Aerial photographs are now captured with digital imaging cameras instead of photographic film plate cameras. This advancement offers more vivid data acquisition than conventional black and white or 3 band colour photographs. Similarly automatic DEM extraction and digital orthophoto generation processes are also now computer based and are saved on computer storage media directly. Consequently digital photogrammetry is sometimes referred to as softcopy photogrammetry. With the development of digital photogrammetry, photogrammetric techniques are now more closely integrated into remote sensing and GIS.

The following sections give brief introduction to types of aerial RS data used in conventional and digital technologies. This explanation will help to understand the technicalities related with RS data quality.

A.2.1. Black and white film

Prior to digital technology, conventional aerial photography used medium to large format cameras capable of recording images on black and white photographs. An advantage of photographic film over human eye is its broadened spectral sensitivity. As a result of which, it can *see* and record over a wavelength range twice as broad (from 0.3μm to 0.9μm) as that of the human eye (0.4μm to 0.7μm). These photographs are normally made with *panchromatic* film or *infra-red sensitive* film which have generalised spectral sensitivities that fall in the ultra violet and the visible spectrum. In the latter case, it also falls in the near infra-red energy, as shown in the Figure 15.

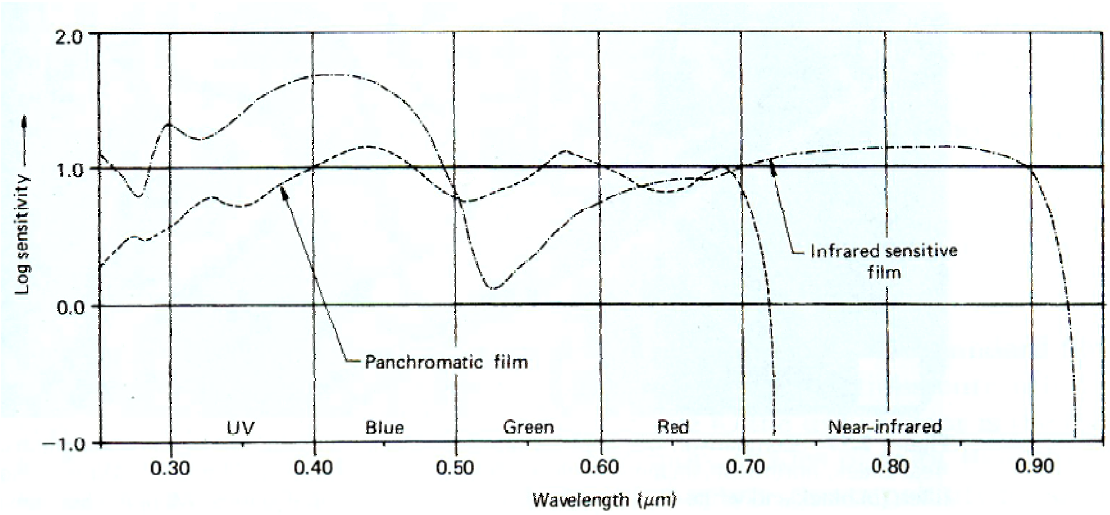

Figure 15: Generalized spectral sensitivities for panchromatic and black and white infrared sensitive films. (Adapted from Lillesand et al., 2004)

A.2.2. Colour film

Although black and white panchromatic film has long been the standard film type for aerial photography, many remote sensing applications currently involve the use of colour film. Colour images enable humans to more easily discriminate many more shades of colour than the tones of gray. A colour film is manufactured with three different light sensitive layers (using colour dyes or pigments) on a film base. These colour dyes result in the selective sensitisation of these layers to the blue, green and red primary colours. The spectral sensitivity of these dye layers is shown in Figure 16.

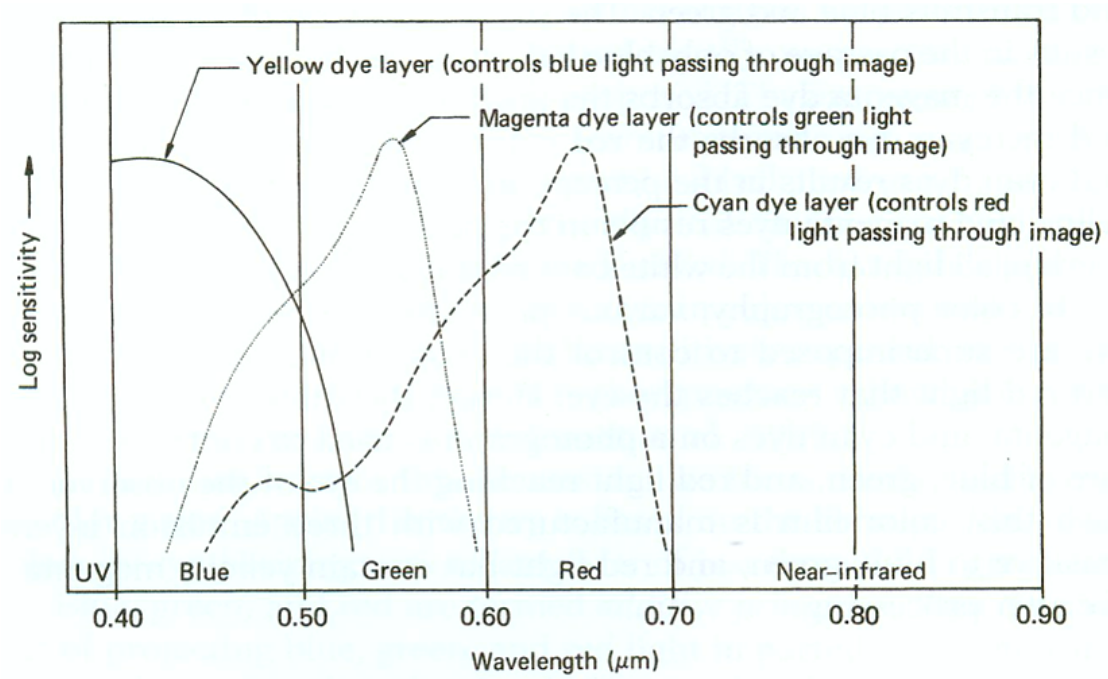

Figure 16: Spectral sensitivity of the three dye layers on a colour film. (Adapted from Lillesand et al., 2004)

In contrast to normal colour film, colour infra-red film (also known as CIR) is manufactured to record green, red and photographic infra-red (0.7μm to 0.9μm) of the

near infra-red scene energy in its three emulsion layers. Spectral sensitivity of CIR is shown in Figure 17.

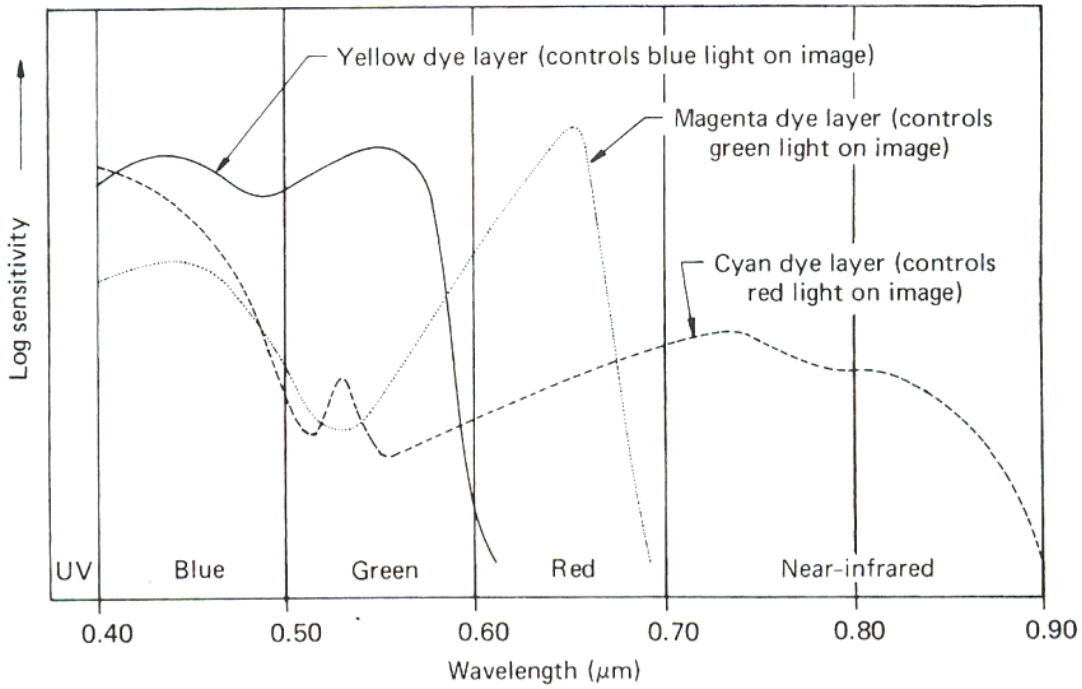

Figure 17: Spectral sensitivity of the three dye layers on a colour IR film.
(Adapted from (Lillesand et al., 2004)

The scale of aerial photographs has traditionally been a measure of the resolution of film-based aerial photography and is calculated as (Avery, 1968):

$$\text{Scale} = \frac{\text{lens focal length}}{\text{camera height AGL}} \quad \text{.....(1)}$$

As scale is a ratio, both of these factors should be in the same units. For example, a camera with a 28mm (or 0.028m) focal length lens flying at an altitude of about 1800m *above ground level* (AGL) will form images with a scale of roughly 1/65,000 (more precisely 1:64,285) on its focal plane.

The resolving ability of a film camera system (or simply film resolution) has been improved considerably in the past forty years. It is measured by the area weighted average resolution (AWAR), in line pairs per millimetre (lp mm^{-1}). The improvement went from 60 lp mm^{-1} to more than 125 lp mm^{-1}. In the case of high altitude photography, its resolving power is achieved up to 630 lp mm^{-1} for high contrast scenes. However, final film resolution is reduced during normal flight surveys, due to atmospheric disturbances and to image blur resulting from the forward and angular motion of the airplane i.e. roll, pitch and yaw (Light, 1996). The effect of scale and film resolution can be combined to express image quality in terms of *ground resolution distance* (GRD) which can be expressed as,

$$\text{GRD} = \frac{\text{reciprocal of image scale}}{\text{film resolution}} \quad \text{..... (2)}$$

This means that at the scale of 1:40,000 and film resolution of 80 lp mm^{-1} for low contrast scenes and 125 lp mm^{-1} for high contrast scenes corresponds to 500mm (or 0.5m) and 320mm (or 0.32m) on the ground, respectively. This image quality and scale can be obtained when Kodak Aerocolor III (negative) film no. 2444 is used at an altitude of 6000m with large format camera (such as Leica-Wild RC 30 camera or Zeiss Top-15 camera), using a focal length of 152mm (Light, 1996; Lillesand et al., 2004).

A.2.3. Digital imaging

Electronic imaging instruments typically use one or two dimensional detector arrays of light sensing solid state devices or photodiodes for image acquisition. Each photodiode has a unique position (known as *photosite*) within an array. These photodiodes are based on either *charge-coupled device* (CCD) or *complementary metal-oxide semiconductor* (CMOS) sensor. CMOS sensor has less light sensitivity and as a result it produces an image with greater noise requiring substantially more image processing time. However, new CMOS technology has substantially overcome this limitation.

These photodiodes are usually square and are arranged in rows and columns within an array while their total number in an array defines the digital image resolution. When electromagnetic energy falls on these photodiodes, it produces electronic charges while magnitude of these charges is proportional to the scene brightness. This information is digitally stored on a recording media (usually on a hard disk) in a raster format. A raster dataset is a two dimensional array of discrete picture elements (known as *pixels*). Each pixel within a dataset represents scene brightness (recorded by the corresponding photosite on CCD or CMOS sensor) in the form of digital number (DN). An ability of a digital sensor to record scene brightness in as many intensity or *quantisation* levels defines its *bit depth* or *radiometric resolution,* which conventionally ranges from 2^8 to 2^{12} bits (256 to 4096 intensity levels). A CCD array with 4008 columns and 2495 rows of photodiodes can generate 10.0 mega-pixel images. Many of CCD or CMOS image sensors used in remote sensing have much better abilities to differentiate a wider range of scene brightness values than most photographic films.

The immediate product of a digital camera is a viewable image, not a negative. The nominal resolution of a digital system is measured as *ground sampled distance* (GSD). This is approximately doubled to compare it with film-based camera system i.e. GRD which means that 1-m resolution digital image will have the approximate detection capability of a 2-m resolution film camera system (Lillesand et al., 2004).

Comer et al. (1998) suggest that if the image in the focal plane is sensed by a CCD array, then the GSD should be calculated as;

$$\text{GSD} = \frac{\text{pixel size} \times \text{camera height AGL}}{\text{lens focal length}} \quad \text{.....(3)}$$

To continue the example mentioned with AP scale (see equation 1), if the array element size is about 0.009mm (9μm) then the GSD is about 0.58m (~2feet).

A.2.4. Digital colour imaging

These CCD images are generally monochromatic which means that there is one photodiode per photosite in an array. In order to generate a colour image, each photodiode of the CCD is covered with a blue, green or red filter. In the conventional digital colour imaging, there is a pattern of alternating rows of blue and red sensitive photosites alongside green sensitive photosites. This is called *Bayer pattern* in which every second photosite is green sensitive in a matrix array while the remaining 50% space is shared equally between blue and red sensitive photosites. To assign blue, green and red values to each photosite, the two missing colours at each photosite are interpolated from the surrounding photosites.

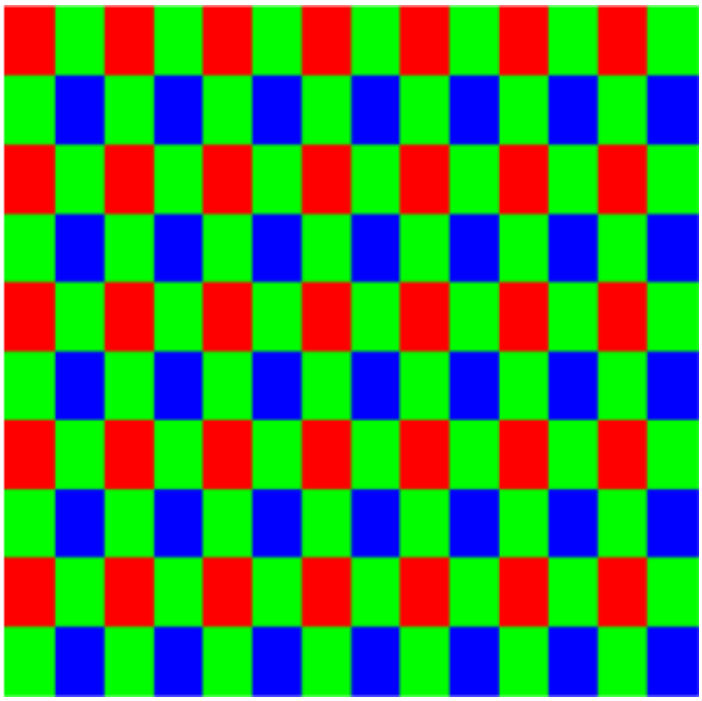

Figure 18: Bayer pattern of blue, green and red CCD (pixel) filters

Advance CCD sensors are available with two photodiodes with a larger primary photodiode with high sensitivity and a secondary smaller photodiode with low sensitivity. Such arrangement provides greater detail in the very bright areas and greater ability to resolve in the dark areas like shadows. Even a three layer CMOS sensor has three photo-detectors (blue, green and red) at every pixel which conceptually results in sharper images with better colours than Bayer pattern matrix CCD.

In advance aerial scanners, a linear array of CCDs is used instead of a two-dimensional (or matrix) array. Linear array CCDs are designed to be very small and can contain over 10,000 individual detectors. Time-Delay Integration (or TDI) is another advanced imaging technique in which rows of pixels are synchronized and transferred at the same motion and rate as the scene. These types of devices are excellent for advanced aerial reconnaissance or applications requiring high speed readout. To make a colour image from these types of arrays, separate linear arrays are required in the blue, green and red parts of the energy spectrum.

A.2.5. Multispectral imaging

In the visual interpretation of remotely sensed images, a variety of image characteristics is brought into consideration: colour (or tone in the case of panchromatic images), texture, size, shape, pattern and context or association. With computer-assisted interpretation, it is most often simply colour that is used to recognise different features. It is for this reason that a strong emphasis is placed on capturing data in multiple discrete spectral ranges. Conventional aerial photography (whether analogue or digital) captures data in a very limited part of the energy spectrum (i.e. 0.3µm to 0.9µm). This is captured as either single broad spectral band (*panchromatic*) or three overlapping spectral bands that operate in the pure visible (*colour*) or in the visible to near infrared (*colour infrared*) part of the electromagnetic energy spectrum. Such cameras offer low colour fidelity.

There are cameras which use a combination of 3 CCD arrays to capture single source electro-magnetic energy simultaneously on these CCD arrays. Such cameras use *dichroic reflective prism* to split single source of light into two differing wavelengths. An arrangement of two dichroic prisms splits light into three different wavelengths which are recorded on 3-CCD array cameras. This mechanism is further explained Figure 19 below.

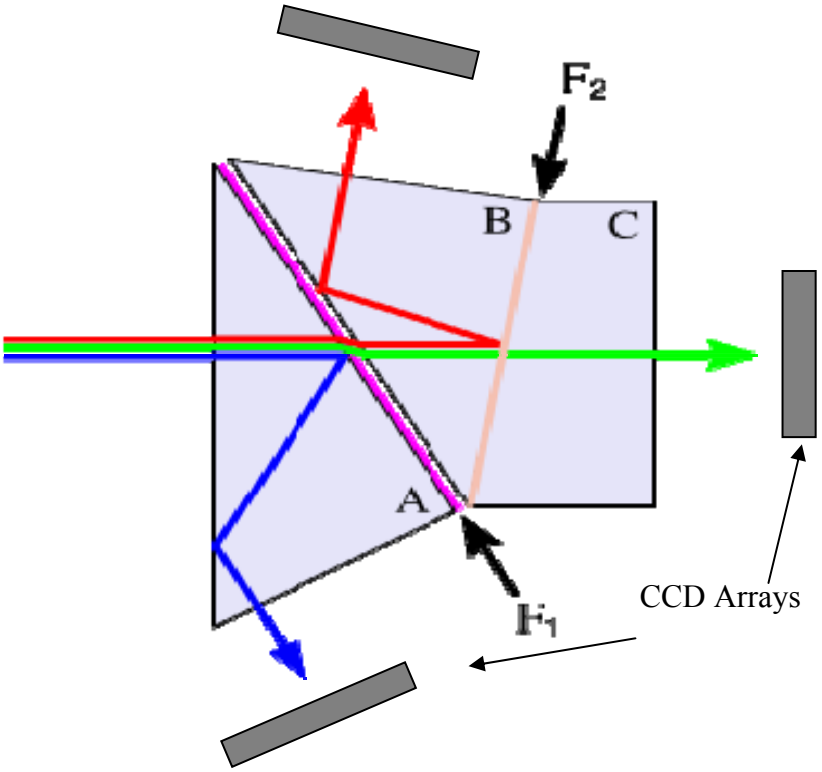

Figure 19: A schematic diagram showing mechanism behind a multispectral array camera, where F1 and F2 are low pass dichroic filters and A, B and C are dichroic prism

The advantage of a multispectral camera is improved colour fidelity which can be further improved in narrow and discrete wavebands if band-pass (BP) filters are used in front of CCD arrays. A band-pass filter allows limited wavelength to transmit through it and attenuating wavelengths beyond its specified upper and lower limits.

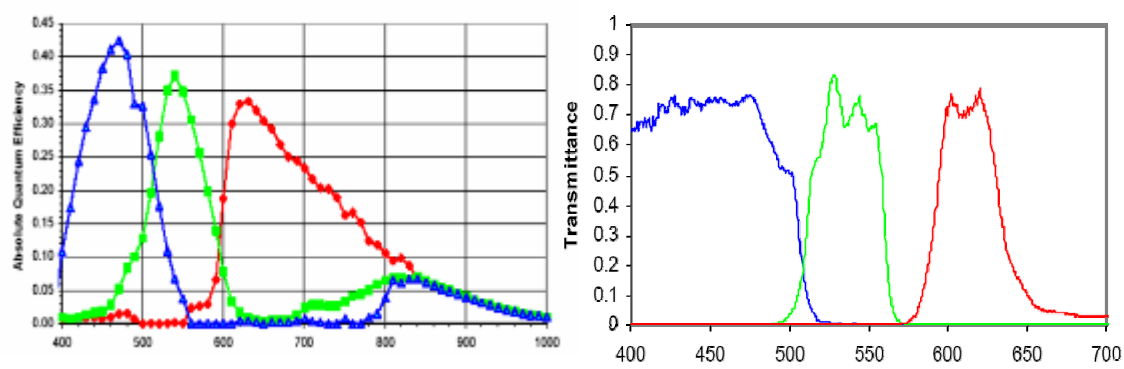

Figure 20: Colour fidelity or response curve for conventional single CCD array camera (right) and multispectral 3-CCD array camera (left)

A.2.6. Thermal imaging

All the objects in the universe radiate energy which is, among other things, a function of surface temperature of the object. As the surface temperature of an object increases, the radiated energy peak shifts to a shorter wavelength. For example, the surface temperature of the sun is 6000K and its peak radiant energy falls within the visible wavelength (at about 0.5µm). Our eyes and photographic films are sensitive to energy of this magnitude and wavelength. However, objects at lower surface temperatures radiate energy at longer wavelengths. For example, the earth's ambient temperature (i.e., the temperature of surface materials such as soil, vegetation and water) is about 300 K (or 27°C) and emits radiation at about 9.7µm. To record this information requires special sensors which are also known as thermographic cameras.

Thermal imaging (also referred to as thermography) produce images of infrared radiation that are beyond the sensitivity level of the human eye or photographic films (roughly 900nm - 14,000nm or 0.9µm - 14µm). Thermographic cameras (sometimes called FLIR or *Forward Looking Infrared*) are essentially infrared thermometers which measure the temperature at many points over a relatively large area to generate a two-dimensional image, with each pixel representing a temperature of the corresponding ground feature.

Quantum or photon detectors are typically used to record radiations in either (or both) 3 to 5µm or 8 to 14µm. In between radiations are heavily absorbed due to the water (H_2O) molecules present in the atmosphere. Mercury-doped Germanium (Ge:Hg) type photon detectors are sensitive to 3 – 14µm spectral range. Others include Indium Antimonide (InSb) or Mercury Cadmium Telluride (MCT or HgCdTe) detectors capable of recording in 3 to 5µm and 8 to 14µm, respectively.

A.2.7. Hyperspectral imaging

Hyperspectral imaging (sometimes refers as spectrometry) covers a similar wavelength range as multispectral systems, but these spectral bands are contiguous with a much narrower wavelength. This dramatically increases the number of bands (typically tens and even hundreds of very narrow bands) in an image. Hyperspectral imaging enables the construction of an effectively continuous reflectance curve for every pixel in the scene and generates an enormous amount of data for image processing, storage and transmission (Becker et al., 2007).

Hyperspectral sensors provide a distinct advantage over multispectral sensors in discriminating such earth features which tend to diagnose absorption and reflection characteristics over narrow wavebands. In traditional multispectral data, this information is usually lost or not significantly recognisable within its relatively coarse spectral bandwidths. Thus, the most common application of hyperspectral imagery is to identify narrow, strategically placed spectral bands for quantifying biophysical characteristics (Becker et al., 2005). This type of remote sensing is very costly and was tested initially with airborne systems. Later, it was introduced on space-borne platforms to offer cheap hyperspectral data, however, it use is limited to study small but diverse regions or features.

A.3. Visualisation of multi-band data

Recent electronic advances have enabled sensors to capture data in discrete but multiple and relatively narrower spectral bands. These bands are not necessarily contiguous in nature which means that the starting value of the next spectral band is not the ending value of the previous spectral band. Such sensors can extend the range of sensing from 0.3 to approximately 14µm which includes ultra violet, blue, green, red, near IR, middle IR and thermal IR parts of energy. All the data captured in different spectral bands appear in the tones of gray like panchromatic data. One of the major advantages of multispectral imaging is its ability to generate vivid images from any three of its spectral bands using the additive mixing principle.

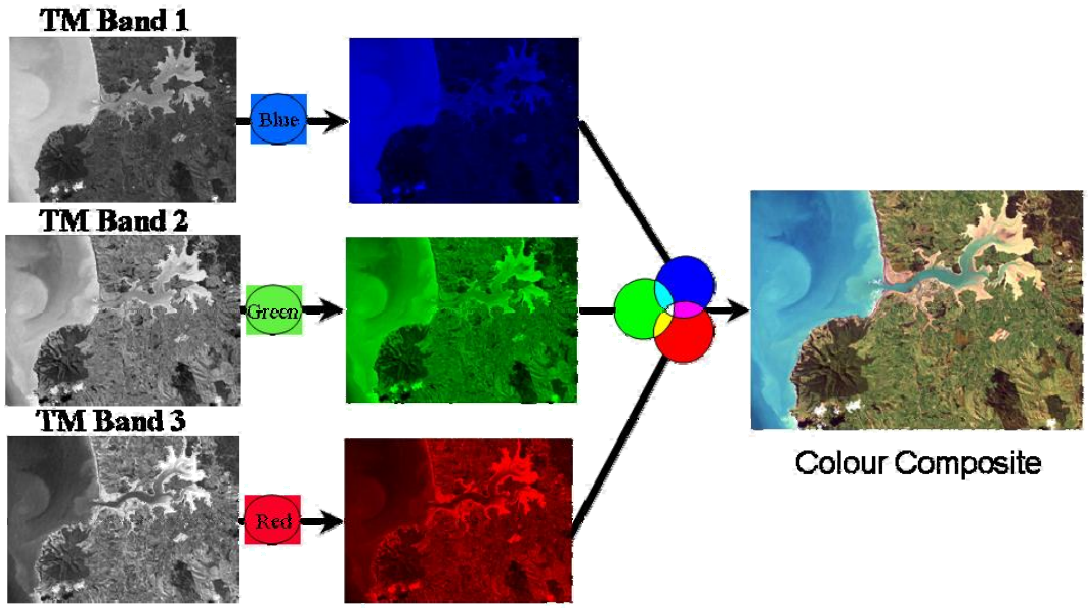

Figure 21: Generation of colour composite using additive mixing of 3 multispectral bands

The best examples of colour additive mixing are *cathode ray tube* (CRT) screens like that of a television or computer monitor. To view data in colour, three spectral bands are shown with the blue, green and red tones of reflectance which are treated as *additive primaries*. A high reflectance of any feature in all three display bands appears white in the colour composite.

A.4. Contemporary airborne systems

With the rise in utility and demand for remote sensing data many commercial airborne sensors are available in the market as ready-to-use products. These are high-priced products which are normally sold as complete airborne system and packaged with bundled hardware and software to carry out data acquisition and its processing. A quick review of these sensors is given to help understand their spatial and spectral characteristics.

It is important to understand that most of the modern aerial scanners use multispectral and hyperspectral imaging technology. Additional advantages include along-track data acquisition and forward- and rear-viewing abilities. The latter provide multiple configurations for stereoscopic base-height ratios.

Along-track scanners use a linear array of CCD or CMOS to generate an image of the features exactly beneath the aeroplane instead of two dimensional framing vertical aerial photographs.

A.4.1. Airborne Data Acquisition and Registration (ADAR)

The Airborne Data Acquisition and Registration (ADAR) System 5500 is an airborne multispectral digital camera system that operates from conventional aerial photography aircraft. The ADAR system hardware includes digital electronic sensors, a global positioning system (GPS) receiver, an onboard computer, real-time video targeting system, and a colour operations console. ADAR collects the imagery digitally using 4 separate sensors. Each sensor records 1500 x 1000 pixels (i.e. 1.5 mega-pixel) within one frame. Visible-blue light, visible-green light, visible-red light, and near-infrared light are recorded simultaneously with the four sensors. Each camera acquires the imagery in 8-bit format (255 levels of reflectance) (Gilvear et al., 2007).

A.4.2. Digital Mapping Camera (DMC)

Intergraph's Z/I Imagining DMC carries 4 high-resolution (7k x 4k) panchromatic camera heads and 4 multispectral (3k x 2k) camera heads on a gyro stabilised camera suspension mount. This is capable of producing high quality panchromatic and multispectral data with ground resolution of less than 5 centimetres (2 inches).

A.4.3. Airborne Digital Sensor (ADS40)

ADS40 is an along-track aerial imaging system manufactured by LH Systems. It is one of the leading airborne scanners and carries multiple linear arrays of CCDs for panchromatic and multispectral image acquisition. All these CCDs share a 62.77mm focal length single lens and captures data in a panchromatic (465-680nm), three visible (430-490nm, 535-585nm, 610-660nm) and one near IR (835-885nm) bands. It carries three linear arrays to capture panchromatic data with one forward-, one nadir- and one rear-viewing at different viewing angles i.e. 28.4° and 14.2° for forward and rear-viewing respectively. Such an arrangement offers three configurations of base-height ratios to generate stereoscopic data. At a typical flying height of 2880m above ground level, it captures data with 15cm ground sample distance (GSD).

A.4.4. Digital Modular Aerial Camera (DIMAC)

DIMAC has a cylindrical camera frame which can carry up to 4 Kodak full-frame CCD colour image sensors with removable filters. Its normal configuration carries conventional blue, green, red and near IR filters to generate multispectral images with 8- or 16-bit radiometric resolution. If it is flown at an altitude of 3000ft with 55mm focal-length lens, it can generate 15cm GSD images. However it has been tested to fly at lower altitude using higher focal-length (120mm) lens that produced up to 2cm resolution images.

Figure 22: Coastal image of Montrevel, France with 15cm GSD showing submerged aquatic vegetation

A.4.5. Airborne Imaging Spectrometer (AIS)

Initial hyperspectral research was conducted with 128 band data acquired by the airborne imaging sensor (AIS). The bandwidth of each spectral band was 9.3nm while

it had only 32 pixel wide image for AIS-1 (later improved to 64 pixels for AIS-2). It had two modes of operation. In "tree-mode", it captured data between 0.4 and 1.2μm while in "rock-mode", it operated between 1.2 and 2.4μm. It was typically operated from an altitude of 4200m above ground, which yielded 8m spatial resolution data.

A.4.6. Compact Airborne Spectrographic Imager (CASI)

CASI was the first commercially developed airborne hyperspectral system and has been available since 1989. A redesigned version (CASI-2) has improved upon the original CASI which enables it to collect data in up to 288 bands between 400 and 950nm at mere 1.8nm bandwidth (Belluco et al., 2006). It is used with GPS, an altimeter and inertial sensors to correct the recorded data for variations in aircraft altitude and attitude (pitch, yaw and roll) during flight. There is an operational trade-off between the number of bands that can be captured and the pixel size at which they are imaged. Increase in the spectral resolution results in low spatial resolution data capture (Becker et al., 2007).

A.4.7. Airborne Visible/Infrared Imaging Spectrometer (AVIRIS)

Airborne Visible/Infrared Imaging Spectrometer (AVIRIS) collects data in 224 bands with 9.6nm bandwidth between 0.4μm and 2.45μm. It has been flown at an altitude of 20km above ground that resulted in 20m spatial resolution data with a 10km swathe.

A.4.8. Reflective Optics System Imaging Spectrometer (ROSIS)

Reflective Optics System Imaging Spectrometer (ROSIS) sensor was developed by DLR Germany, and acquires data in 115 spectral bands in the visible and near infrared part of the spectrum between 415.5 and 875.5nm with a band width of 4nm (Belluco et al., 2006).

A.4.9. Multispectral Infrared & Visible Imaging Spectrometer (MIVIS)

Multispectral Infrared and Visible Imaging Spectrometer (MIVIS) sensor covers data in contiguous bands but within selected wavelength ranges of the energy spectrum. These ranges are from 433 to 833nm (20 spectral bands at 20nm bandwidth); from 1150 to 1550nm (8 spectral bands at 50nm bandwidth); from 2000 to 2500nm (64 spectral bands at 8nm bandwidth) and from 8200nm to 12,700nm (10 bands at 400 to 500nm resolution) (Belluco et al., 2006).

A.5. Passive remote sensing satellites and sensors

The satellite era started on October 4, 1957 with the launch of first artificial satellite (Sputnik) by Soviet Union. From a modest sphere of aluminium, which measured 58cm in diameter and weighed hardly more than 80kg, satellites grew bigger in sizes and diversified in applications. Within just 50 years, approximately 3,000 satellites of all sorts revolved around the Earth out of which earth observation satellites make a substantial contribution.

Satellite remote sensing came almost 20 months after the launch of first artificial satellite when US sent CORONA photographic film camera on-board the KH (Key

Hole) series satellites. Soviet Union followed this development and captured high resolution photographs using KVR-1000 camera on board different satellites. This brought in a paradigm shift in the field of remote sensing. Although these datasets were part of the military reconnaissance, their limited access engaged both the nations in improving this technology. After the break up of Soviet Union in 1994, KVR-1000 data quietly went in the public domain. The US also declassified their data to the general public in 1996 which can be ordered today as scanned images from the original photographic plates.

A noticeable revolution in the satellite remote sensing technology was observed when the US launched its first of *Earth Resources Technology Satellites* (ERTS-1) in July 1972 thus providing the first digital image at 79m spatial resolution for the civilian applications. This programme was renamed Landsat prior to the launch of the second satellite of the series in January 1975. After a decade, the US significantly improved the spatial resolution by adding TM sensor at 30m onboard Landsat-4 in 1982. In less than 3 years, the US launched its fifth of the Landsat series satellite on March 1, 1985 which is the longest serving remote sensing satellite in the history of satellite remote sensing. It is predicted to serve until 2010. The Soviet Union continued capturing images of different parts of the globe in a non-digital fashion. Their first digital image capable satellite was Resurs-O1 which launched in 1985.

About this time other nations also realised the importance of satellite remote sensing data and its commercial significance. Many nations started exploring the potential of earth observation using satellite remote sensing including France, India, Japan and China. Considerable contribution towards satellite remote sensing came from France who launched Spot-1 satellite in 1986. Spot-1 had certain advantages over other RS satellites previously launched by the US and Soviet Union. Its 10m resolution panchromatic band was not only the highest spatial resolution digital sensor but it was also capable of taking across-track stereoscopic images. This technique had a major disadvantage of time delay in capturing the same area from two different orbits. Although, this topic is of least interest to our application, it is significant to know that the Germans experimented with MOMS-2 sensor onboard Mir Space Station in 1993. It was capable of taking forward, nadir and backward images in the along-track fashion. This technique is now implemented as a standard procedure to make stereoscopic DEM from many newly launched satellites like US Terra, French SPOT-5, Indian CartoSat and Japanese ALOS.

India launched IRS-1C in 1995 with the highest spatial resolution data (5.8m) of its time in the public domain. However, the major achievement in spatial resolution was attained with the launch of 1m panchromatic band onboard IKONOS-2 satellite in 1999. The journey towards improving the spatial resolution is ongoing. The first sub-metre resolution (0.6m) digital image was available with the launch of QuickBird-2 satellite in Oct 2001 which is likely to improve further (0.41m) later in this year with the launch of WorldView-1 and GeoEye-1 satellites.

Now with the advancement in the field of electronics and an improved know-how developed in terms of design and of assembly of satellites, a new era of relatively in-expensive micro-satellites (weighing less than 100kg) has begun. In addition to this, experimentation has been conducted to launch nano-satellites (weighing up to 12kg).

As all these satellites carry sensors different from each other in terms of spatial, spectral, radiometric and temporal resolution, it is worthy to note that each satellite and its onboard sensor(s) have some unique characteristics which make it useful for a particular kind of resource mapping.

At present, there are many instruments which are available for image acquisition from both commercial and government organisation operated satellites (for details see *Appendix B*). These sensors enable the collection of data at spatial resolutions ranging from centimetres to kilometres and spectral resolutions ranging from a few broad bands to hundreds of narrow bands on hyperspectral detectors.

There is a long list of RS satellites which have been launched and failed during or after their launch, or decommissioned after serving for a while and decayed. In the past, Earth observation was primarily carried out by state run organisations but in the last decade, satellite remote sensing has been established as a commercial entity. As a result, many private companies are involved in this business. The following section highlights significant earth observation satellites and a brief description of their onboard sensors. To provide ease in understanding, these satellites have been grouped based on their principal operator. For the detailed specifications about their data quality, please refer Appendix B.

A.5.1. Landsat programme

Although the Landsat programme was originally conceived in 1965, the first satellite of this series was launched in 1972. It was the first Earth observation satellite with digital data acquisition capability and data was available to the general public through the National Aeronautics and Space Administration (NASA). The other participants of the project were US Geological Survey (USGS) and General Electric's space division. Earlier series satellites (Landsat-1, -2, -3) carried relatively low spatial resolution sensors like Return Beam Vidicon (RBV) camera and Multi Spectral Scanner (MSS).

By the time Landsat-4 was launched in 1982, Landsat programme was also privatised to a newly formed Earth Observation Satellite (EOSAT) Company. The scope of the monitoring was extended and National Oceanic and Atmospheric Administration (NOAA) also joined the participants list. A new sensor called *Thematic Mapper* (TM) was introduced with 30m spatial resolution. It was capable of looking into seven discrete reflectance bands ranging from visible to thermal infrared. A similar TM sensor onboard Landsat-5 was launched in 1984. Its improved versions, Enhanced Thamatic Mapper (ETM) onboard Landsat-6 and Enhanced Thematic Mapper Plus (ETM+) onboard Landsat-7, either failed during launch or, in the case of the latter sensor, malfunctioned in the year 2003. These sensors had an additional panchromatic band at 15m resolution in addition to improved resolution for TIR. Currently, Landsat programme is operated by USGS. Its TM sensor is the longest serving sensor in the history of earth observation satellites and is expected to continue its data acquisition till 2010. Landsat Data Continuity Mission (LDCM) satellite is expected to be launched in 2011.

The strength of TM sensor is its highest temporal resolution. The same data is available from the last 25 years, and this makes it the best choice for change

monitoring studies. Its spectral range offers blue band to study water related habitat and its wider swathe (185km) enables it to capture larger regions in less number of scenes. The latter factor significantly saves time compared to processing small scenes which usually have seasonal variations.

A major weakness of this sensor is its coarser spatial resolution. Although advance mathematical algorithms are established, the pixel resolution is very coarse for detecting vegetation along narrow river margins.

A.5.2. French satellites

In early 1978, the French government decided to undertake the development of the SPOT programme. It was designed by the French Centre National d'Etudes Spatiales (CNES). Its first satellite (SPOT-1) was launched in 1986. Since then a total of 5 satellites have been launched. It was the first CCD array based satellite. Spot-1 and -2 carried High Resolution Visible (HRV) sensors which were capable of capturing data in green, red and NIR parts of the energy spectrum at 20m spatial resolution. It was also capable of taking data in a panchromatic mode at 10m resolution. In Spot-3 and -4, its improved High Resolution Visible and Infra-red (HRVIR) sensor is capable of looking into the middle infrared zone as well.

In 2002, SPOT-5 (latest SPOT satellite) was launched. This carries a High Resolution Geographic (HRG) sensor, with the same spectral resolution as SPOT 4. However, the spatial resolution of multispectral data is improved to 10m for visible and NIR bands while middle IR band resolution is kept the same (20m). There are two CCDs used for panchromatic data at 5m resolution. These CCDs are placed so that data captured from the second CCD has a half pixel off-set from the first data. During processing at the ground station, the data captured by these CCDs are interlaced and interpolated to generate 2.5m resolution panchromatic images.

The strength of HRG data is its spatial resolution i.e. 2.5m and 10m for panchromatic and multispectral bands respectively. The swathe of Spot data is 60km and has been successfully used for national level mapping. To use in monitoring freshwater habitats, the significant drawback of this sensor is its inability to look in the blue wavelength. It is also expensive.

A.5.3. Indian satellites

Indian Space Research Organisation (ISRO) has launched many RS satellites with success in the past. Like SPOT series, these satellites also carry a similar type of sensor which improved their spatial accuracy over the period of time. The first satellite IRS (Indian Remote sensing Satellite)-1A was launched in 1988. It carried two sensors - Linear Imaging Self-scanning Sensor (LISS) -I and -II, which were roughly equivalent to Landsat TM in spectral response but were capable of data capture in the first four spectral bands i.e. in blue, green, red and near IR. Their spatial resolutions were 72.5m and 36.25m. These sensors were repeated on IRS-1B, but IRS-1C and -1D in 1995 and 1997 carried the LISS-III sensor along with two additional sensors i.e. Panchromatic and WiFS (Wide Field Sensor). LISS-III, although having improved spatial resolution up to 23metres, had the blue wavelength capable spectral band replaced with 70m resolution middle IR band. The

panchromatic sensor is able to capture data at 5.8m resolution while WiFS can sense at much coarser resolution (188m) in only two spectral ranges (i.e. red and near IR).

In 2003, a new satellite of its series was launched. The IRS-6P or ResourceSat carries a similar LISS-III sensor along with new and improved LISS-IV and AWiFS (Advance Wide Field Sensor) sensors with 5.8m and 56m spatial resolutions respectively. These three sensors carry similar spectral wavelength bands in green, red, near IR and middle IR parts of the energy spectrum. In LISS-IV, the middle IR band is dropped out at the expense of panchromatic sensor which can capture data at the same spatial resolution but its swathe is 70km as compared to multispectral LISS-IV data (i.e. 23km).

The major strength of this satellite is its ability to sense objects in the same spectral range across different sensors. There is also a high degree of spatial variability i.e. 5.8m, 23m and 56m for LISS-IV,-III and AWiFS sensors respectively. AWiFS is the widest swathe (740km) sensor among other medium spatial resolution sensors which makes it a good choice for large scale studies such as water quality mapping for the entire Waikato region.

The spectral resolution for LISS-IV is 10 bits which is good among its other competitor satellites such as SPOT and ALOS. However, its narrow swathe (23km) is a major disadvantage to use for regional scale monitoring studies. LISS-III has low radiometric and temporal resolution i.e. 7 bits and 24 days, respectively.

A.5.4. NASA satellites

The National Aeronautics and Space Administration (NASA) is familiar for its space exploration experimentations. Earth Observing System (EOS) is NASA's important component that deals with development of new tools to monitor earth. Terra satellite was launched in 1999 with the collaboration of Japan's Ministry of International Trade and Industry. Its onboard sensor for the earth observation is called ASTER (Advance Space-borne Thermal Emission and Reflection Radiometer) which provides imaging data in 14 spectral bands. ASTER consists of three separate instrument subsystems, operating in different spectral regions. These subsystems are Visible and Near Infrared (VNIR), Short Wave Infrared (SWIR) and Thermal Infrared (TIR) with 15m, 30m and 90m ground resolutions.

The National Aeronautics and Space Administration's EO-1 satellite was launched on November 21, 2000 as part of a one-year technology validation/demonstration mission. The Advanced Land Imager (ALI) instrument on EO-1 was used to validate and demonstrate technology for the Landsat Data Continuity Mission (LDCM). The original EO-1 mission was successfully completed in November 2001. As the end of the mission approached, the remote sensing research and scientific communities expressed high interest in continued acquisition of image data from EO-1. Based on this user interest and willingness to assist in funding continued operations, an agreement was reached between NASA and the United States Geological Survey (USGS) to allow continuation of the EO-1 program as an 'extended mission'. It carries two sensors, Advance Land Imaging (ALI) and Hyperion sensors. In contrast to TM or ETM+, ALI employs push broom scanning and features 10m panchromatic

and 30m multispectral image acquisition. The ALI bands are designed to mimic ETM+ bands with three additional bands in blue and near IR region.

The Hyperion sensor onboard EO-1 is the first space borne hyperspectral sensor which captures data in 242 spectral bands. During level 1 processing of its data; only 198 bands out of 242 are calibrated as others exhibit poor signal-to-noise ratio. The ground resolution of this experimental sensor is 30m while swathe is extremely narrow i.e. 7.7km.

The major strengths of ASTER sensor are its low cost, higher spatial resolution and wider swathe i.e. 60km. However, it does not capture data in blue wavelength. ALI offers better spectral resolution with 4 bands in visible spectrum. The disadvantages are its low spatial resolution, and lack of planned and routine acquisition. Hyperion is an experimental sensor with a small footprint (7.7 × 185km) and the data is not collected routinely. Therefore, it is not suitable for regular near-real time monitoring (Reinart and Kutser, 2006).

A.5.5. European space agency satellites

In March 2002, the European Space Agency (ESA) launched Envisat-1, an advanced polar-orbiting Earth observation satellite which provides measurements of the atmosphere, ocean, land, and ice. Besides other sensors, the Envisat satellite carries MERIS (medium resolution imaging spectrometer). The MERIS is a push-broom instrument having 1150km wide swathe while ground resolution of data is 300m. It is a programmable sensor with fifteen spectral bands which can be selected by ground command, each of which has a programmable width and a programmable location in the 390nm to 1040nm spectral range.

The Project for On-Board Autonomy (PROBA) satellite was originally a technology demonstration mission of the European Space Agency, launch on 22nd Oct 2001. It carries two Earth Observation instruments CHRIS and HRC.

Compact High Resolution Imaging Spectrometer (CHRIS) is the prime instrument of the PROBA mission and a hyperspectral sensor. It is used to measure directional spectral reflectance of land areas, thus providing new biophysical and biochemical data, and information on land surfaces. It provides multiple imaging of the same target area under different viewing and illumination geometries. Its spectral range is between 415 to 1050nm while band width varies between 5 to 12nm and it can capture data within up to 19 spectral bands. Its spatial resolution is 20m at nadir and its swathe width is 14km.

HRC (High resolution camera) is a black and white camera with a 1024 x 1024 (1 mega pixel) CCD array and a miniaturised telescope. With a high spatial resolution of five metres, HRC can acquire images with an area of 25 square kilometres.

A.5.6. Japanese satellites

Japan has launched few earth observation satellites in the past. This includes MOS (Marine Observation Satellite)-1 and -1b in 1987 and 1990; JERS (Japan Earth Resources Satellite)-1 in 1992 and ADEOS (Advance Earth Observing Satellite) in

1996. These satellites carried Multispectral Electronic Self-scanning Radiometer (MESSR), OPS (Optical Sensor) and Advance Visible and Near Infrared Radiometer (AVNIR) sensors respectively. More considerable among these sensors is AVNIR whose improved sensor (AVNIR-2) was recently launched on ALOS (Advance Land Observation Satellite) in 2006. This sensor captures data in four multispectral bands and operates in blue, green, red and NIR wavelengths. Another sensor onboard ALOS is Panchromatic Remote Sensing Instrument for Stereo Mapping (PRISM) which captures data in 2.5m ground resolution in nadir, for-ward and aft-ward viewing.

The strengths of this satellite are its wider swathe i.e. 70km data at 2.5m resolution, low cost and ability to look in blue band. These advantages provide great opportunities to study aquatic habitats. One should not forget that this satellite is recently launched and holds a limited data archive for NZ.

A.5.7. High resolution commercial satellites

The first successful launch of a commercially developed high resolution earth observation satellite happened with the launch of IKONOS-2 satellite in 1999. Its successful launch and public interest in high resolution imagery opened a new dimension for the satellite remote sensing industry. It was capable of acquiring images at 4m multispectral and 1m panchromatic bands. It has a narrow swathe of 11km and thus requires a long time to capture one time data for the entire globe. Later QuickBird-2 and OrbView-3 filled this gap after their launch in 2001 and 2003 respectively. OrbView-3 has similar spatial resolution as IKONOS-2 but QuickBird-2 offered 0.61m and 2.4m resolution panchromatic and multispectral data. All these satellites capture data in blue, green, red and NIR bands and thus provide good opportunities to study macrophytes in the aquatic habitat. Even higher resolution sensors have been announced by these companies and 0.41m resolution image is expected in late 2007.

A.6. Discussion

There are distinct advantages of digital technology over conventional photography. Digital cameras utilize light-sensitive computer chip (CCD) technology to acquire photographic imagery rather than conventional film emulsion. Malthus and Mumby (2003) suggest that digital imaging reduces the need for survey film, processing chemicals and printing paper, which in turn significantly reduces costs. Digitally captured multi-spectral images typically offer superior spectral fidelity when compared to images scanned from colour infrared film. However, the quality of current digital imaging is at-par with small to medium format films and cannot challenge large format 230mm films (Muller, 1997). With a linear array used in a push-broom scan mode, an array of 21000 detectors would be necessary to retain the spatial integrity of large format films. The current capacity of the CCD array is in the range of 5000 detectors. The production of sufficiently large CCD arrays is impossible at the moment, so large-format digital cameras are built either as multi-head systems by fusing several smaller CCD arrays and cameras or by using linear CCD arrays (Honkavaara et al., 2006). Some of the airborne sensors discussed above have used two parallel detectors to increase the area of acquisition.

The comparison above of conventional aerial photography with current digital imaging is primarily for accuracy levels associated with topographic maps at a large scale (i.e. 1:50,000 and below). Our prime concern is to see whether digital imaging offers us the opportunity to perform localised monitoring of riparian and littoral habitats. The real challenges of the airborne digital imaging data, as described by Malthus and Mumby (2003) over littoral and sub-littoral regions are (i) the need to convert radiance to reflectance in order to develop a mosaic of imagery along adjacent flight lines; and (ii) the need for accurate geometric correction of the data given the potential absence of verifiable ground control points over major parts of the imagery. The second argument has more weight for the mapping of large water bodies.

Within satellite based sensors, not every sensor offers the same set of data quality. It is necessary to match data quality with end use application. There are trade offs between spatial, spectral, and radiometric resolution which are taken into consideration when designing a sensor. For high spatial resolution, the sensor has to have a small IFOV (Instantaneous Field of View). However, this reduces the amount of energy that can be detected as the area of the ground resolution cell within the IFOV becomes smaller. This leads to reduced radiometric resolution - the ability to detect fine energy differences. To increase the amount of energy detected (and thus, the radiometric resolution) without reducing spatial resolution, we would have to broaden the wavelength range detected for a particular channel or band. Unfortunately, this would reduce the spectral resolution of the sensor. Conversely, coarser spatial resolution would allow improved radiometric and/or spectral resolution. Thus, these three types of resolution must be balanced against the desired capabilities and objectives of the sensor.

The development of a CCD array camera that offers spectral resolution of more than 3 distinct spectral bands may be useful for this project. Such development can significantly improve the capacity to not only map riparian and littoral habitats for the first time but will ensure regular data acquisition using similar spectral and spatial parameters.

Appendix B: Past & Current Digital Passive Sensors (of spatial res 250m and better) onboard Sun-synchronous EO Satellite Systems

Sr. No.	Satellite (Country)	Launched	De-commissioned/ Failed/ Malfunctioned	Sensor(s)	Spectral Resolution				Spatial Resolution		Radiometric Resolution (bits)	Temporal Resolution (days)
					No. of bands, band nos. & spectral range (µm)				Pixel size (m)	Swathe (km)		
1	Landsat-1 or ERTS-1 (USA)	July 23, 1972	Jan 6, 1978	MSS	4	Visible	B4	0.50 – 0.60	79	185	8	18
							B5	0.60 – 0.70				
						NIR	B6	0.70 – 0.80				
2	Landsat-2 (USA)	Jan 22, 1975	Feb 25, 1982				B7	0.80 – 1.10				
3	Landsat-3 (USA)	Mar 5, 1978	Mar 31, 1983			TNIR[i]	B8	10.4 – 12.6	240			
4	Landsat-4 (USA)	Jul 16, 1982	Jun 15, 2001	MSS	Same spectral details as MSS sensor onboard Landsat-1 or -2[ii]				82	185	8	16
			Aug 1993	TM	7	Visible	B1	0.45 – 0.52	30			
							B2	0.52 – 0.60				
							B3	0.63 – 0.69				
						NIR	B4	0.76 – 0.90				
						SWIR	B5	1.55 – 1.75				
							B7	2.08 – 2.35				
						TNIR	B6	10.4 – 12.5	120			
5 (1)[iii]	Landsat-5 (USA)	Mar 01, 1984	Aug, 1995[iv]	MSS	Same spectral details as MSS sensor onboard Landsat-1, -2 or -4							
			Operational	TM	Same spectral details as TM sensor onboard Landsat-4							

[i] Thermal IR band was introduced in the Landsat-3 mission which failed shortly after launch
[ii] MSS bands in Landsat-4 and -5 were renumbered as Band 1, 2, 3, and 4
[iii] The number in parenthesis shows the order of the currently operational satellite
[iv] MSS sensor was powered off in 1995 while TM sensor is expected to run until 2010

Sr. No.	Satellite (Country)	Launched	De-commissioned/ Failed/ Malfunctioned	Sensor(s)	Spectral Resolution				Spatial Resolution		Radiometric Resolution (bits)	Temporal Resolution (days)
					No. of bands, band nos. & spectral range (µm)				Pixel size (m)	Swathe (km)		
6	Resurs-O1 N1 or Cosmos 1689 (Soviet Union)	Oct 03, 1985	Nov, 1986[v]	2xMSU-E	3	Visible	B1	0.50 – 0.59	45	45	?	?
							B2	0.61 – 0.69				
						NIR	B3	0.81 – 0. 90				
				MSU-S	2	Visible	B1	?	240	1380	?	?
						NIR	B2	?				
				MSU-SK	5	?	B1	?	170	600	?	?
						?	B2	?				
						?	B3	?				
						?	B4	?				
						TIR	B5	10.4 – 12.6	600			
7	SPOT-1 (France)	Feb 22, 1986	Nov 28, 2003	HRV-1 HRV-2	4	Pan	PAN	0.49 – 0.69	10	60	8	5 - 26[vi]
						Visible	XS1	0.49 – 0.61	20			
							XS2	0.61 – 0.68				
						NIR	XS3	0.78 – 0.89				
8	Momo-1 or MOS-1[vii] (Japan)	Feb 19, 1987		MESSR[viii]	4	Visible	B1	0.51 - 0.59	50	100	?	?
							B2	0.61 – 0.69				
						NIR	B3	0.72 – 0.80				
							B4	0.80 – 1.10				
9	IRS-1A (India)	Mar 17, 1988		LISS-I	4	Visible	B1	0.45 – 0.52	72.5	148	7	22
							B2	0.52 – 0.59				
							B3	0.62 – 0.68				
						NIR	B4	0.77 – 0.86				
				LISS-II a LISS-II b	4	Visible	B1	0.45 – 0.52	36.25	145		
							B2	0.52 – 0.59				
							B3	0.62 – 0.68				
						NIR	B4	0.77 – 0.86				
10	Resurs-O1 N2 or (Soviet Union)	Apr 20, 1988	Oct 1994	2xMSU-E	Same as Resurs-O1 N1							
				2xMSU-SK								
11 (2)	SPOT-2 (France)	Jan 22, 1990	Operational	HRV-1 HRV-2	Same spectral details as HRV sensor onboard Spot-1							

[v] Re-entered the earth's orbit on Jan 14, 2001
[vi] Revisit time is reduced up to 5 days due to its side viewing capability
[vii] Marine Observation Satellite
[viii] Multispectral Electronic Self-Scanning Radiometer

Sr. No.	Satellite (Country)	Launched	De-commissioned/ Failed/ Malfunctioned	Sensor(s)	Spectral Resolution				Spatial Resolution		Radiometric Resolution (bits)	Temporal Resolution (days)
					No. of bands, band nos. & spectral range (µm)				Pixel size (m)	Swathe (km)		
12	MOS-1b (Japan)	Feb 2, 1990	May 19, 1996	Same spectral details as MESSR sensor onboard MOS-1								
13	IRS-1B (India)	Aug 29, 1991		LISS-I LISS-II a, b	Same spectral details as LISS-I and -II onboard IRS-1A							
14	*Foyu-1 or JERS-1* (Japan)	Feb 11, 1992	1998	OPS[ix]	7	Visible	B1	0.52 – 0.60	18 x 24	75		44
							B2	0.63 – 0.69				
						NIR[x]	B3	0.76 – 0.86				
						SWIR	B4	1.60 – 1.71				
							B5	2.01 – 2.12				
							B6	2.13 – 2.25				
							B7	2.27 – 2.40				
15	Spot-3 France	Sep 26, 1993	Nov 14, 1996	HRVIR-1 HRVIR-2	5	Pan	PAN	0.49 – 0.69	10	60	8	5 – 26[vi]
						Visible	XS1	0.49 – 0.61	20			
							XS2	0.61 – 0.68				
						NIR	XS3	0.78 – 0.89				
						SWIR	XS4	1.58 – 1.75				
16	Landsat-6 (USA)	Oct 05, 1993	Failed during launch	ETM	8	Pan	B8	0.50 – 0.90	15	185	8	
						Visible	B1	0.45 – 0.52	30			
							B2	0.52 – 0.60				
							B3	0.63 – 0.69				
						NIR	B4	0.76 – 0.90				
						SWIR	B5	1.55 – 1.75				
							B7	2.08 – 2.35				
						TIR	B6	10.4 – 12.5	120			
17	IRS-P2 (India)	Oct 15, 1994		LISS-II a,b	Same spectral details as LISS-II onboard IRS-1A and -1B							

[ix] Optical Sensor
[x] The following band had along track stereoscopic coverage capability

Sr. No.	Satellite (Country)	Launched	De-commissioned/ Failed/ Malfunctioned	Sensor(s)	Spectral Resolution				Spatial Resolution		Radiometric Resolution (bits)	Temporal Resolution (days)
					No. of bands, band nos. & spectral range (µm)				Pixel size (m)	Swathe (km)		
18	Resurs-O1 N3 (Russia)	Nov 04, 1994	Sep 11, 1998	MSU-E	3	Visible	B1	0.50 – 0.59	35		45	
							B2	0.61 – 0.69				
						NIR	B3	0.81 – 0. 90				
				MSU-SK	5	Visible	B1	0.50 – 0.60	140		600	
							B2	0.60 – 0.70				
						NIR	B3	0.70 – 0. 80				
							B4	0.80 – 1.00				
						TIR	B5	10.4 – 12.6				
19 (3)	IRS-1C (India)	Dec 28, 1995	Operational	Pan		1	PAN	0.50 – 0.75	5.8	70	6	22
				LISS-III	4	Visible	B1	0.52 – 0.59	23.5	142	7	
							B2	0.62 – 0.68				
						NIR	B3	0.77 – 0.86				
						SWIR	B4	1.55 – 1.75	70.5	148		
				WiFS	2	Visible	B1	0.62 – 0.68	188	810		5
							B2	0.77 – 0.86				
20	IRS-P3 India	Mar 21, 1996	Decommissioned??	LISS II	Same spectral details as IRS-1A							
21	ADEOS[xi] (Japan)	Aug 17, 1996	Feb 1997	AVNIR	5	Pan	PAN	0.52 – 0.59	8	80		
						Visible	B1	0.42 – 0.50	16			
							B2	0.52 – 0.60				
							B3	0.61 – 0.69				
						NIR	B4	0.76 – 0.89				
22 (4)	IRS-1D (India)	Sep 29, 1997	Operational	Pan	Same spectral details as IRS-1C							
				LISS-III								
				WiFS								
23 (5)	Spot-4 (France)	Mar 24, 1998	Operational	HRVIR-1 HRVIR-2	5	Pan	PAN	0.49 – 0.69	10	60	8	5 – 26[vi]
						Visible	XS1	0.49 – 0.61	20			
							XS2	0.61 – 0.68				
						NIR	XS3	0.78 – 0.89				
						SWIR	SWIR	1.58 – 1.75				
24	Resurs-O1 N4 (Russia)	Jul 10, 1998	Decommissioned??	MSU-E	Same spectral details as Resurs-O1 N3							
				MSU-SK								

[xi] ADvance Earth Observation Satellite

Sr. No.	Satellite (Country)	Launched	De-commissioned/ Failed/ Malfunctioned	Sensor(s)	Spectral Resolution				Spatial Resolution		Radiometric Resolution (bits)	Temporal Resolution (days)
					No. of bands, band nos. & spectral range (µm)				Pixel size (m)	Swathe (km)		
25 (6)	Landsat-7 (USA)	Apr 15, 1999	[xii]	ETM+	8	Pan	B8	0.50 – 0.90	15	185	8	16
						Visible	B1	0.45 – 0.52	30			
							B2	0.52 – 0.60				
							B3	0.63 – 0.69				
						NIR	B4	0.76 – 0.90				
						SWIR	B5	1.55 – 1.75				
							B7	2.08 – 2.35				
						TIR	B6	10.4 – 12.5	60			
26 (7)	IKONOS-2 (USA)	Sep 24, 1999		Pan	1	Pan	PAN	0.45 – 0.90	1	11.3	11	5
				Multi-spectral	4	Visible	B1	0.45 – 0.52	4			
							B2	0.51 – 0.60				
							B3	0.63 – 0.70				
						NIR	B4	0.76 – 0.85				
27	CBERS-1 (China / Brazil)	Oct 14, 1999	???	HRCC[xiii]	5	Pan	B5	0.510 – 0.730	20	113		3 – 26
						Visible	B1	0.420 – 0.520				
							B2	0.520 – 0.590				
							B3	0.630 – 0.690				
						NIR	B4	0.770 – 0.890				
				IRMSS[xiv]	4	Pan	PAN	0.500 – 1.100	80	120		26
						NIR	B1	1.550 – 1.750				
							B2	2.080 – 2.350				
						TIR	B3	10.40 – 12.50	160			
				WFI[xv]	2	Visible	B1	0.630 – 0.690	260	890		5
						NIR	B2	0.770 – 0.890				

[xii] Scan Line Corrector (SLC) malfunctioned on May 31, 2003 resulted in the onward acquisition of down graded data
[xiii] High Resolution CCD Camera
[xiv] IRMSS – Infra-Red Multi-Spectral Scanner
[xv] WFI – Wide Field Imager

Sr. No.	Satellite (Country)	Launched	De-commissioned/ Failed/ Malfunctioned	Sensor(s)	Spectral Resolution				Spatial Resolution		Radiometric Resolution (bits)	Temporal Resolution (days)
					No. of bands, band nos. & spectral range (µm)				Pixel size (m)	Swathe (km)		
28 (8)	TERRA or EOS AM-1 (USA/Japan)	Dec 15, 1999		ASTER	14	Visible	B1	0.52 – 0.60	15	60	8	16
							B2	0.63 – 0.69				
						NIR	B3 nadir	0.78 – 0.86				
							B3 back					
						SWIR	B4	1.6 – 1.0	30			
							B5	2.145 – 2.185				
							B6	2.185 – 2.225				
							B7	2.235 – 2.285				
							B8	2.295 – 2.365				
							B9	2.360 – 2.430				
						TIR	B10	8.125 – 8.475	90		12	
							B11	8.475 – 8.825				
							B12	8.925 – 9.275				
							B13	10.25 – 10.95				
							B14	10.95 – 11.65				
				MODIS	36	Visible	B1	0.62 – 0.67	250	2330		2
						NIR	B2	0.841 – 0.874				
						5	B3-7	V, NIR, SWIR	500			
						29	B8-36	V, N, SW, TIR	1000			
29 (9)	KOMPSAT-1[xvi] or Arirang-1 (South Korea)	Dec 20, 1999		EOC[xvii]	1	Visible	PAN	0.51 – 0.73	6.6	17	8	

[xvi] KOMPSAT – Korean Multi-Purpose Satellite
[xvii] EOC – Electro-Optical Camera

Sr. No.	Satellite (Country)	Launched	De-commissioned/ Failed/ Malfunctioned	Sensor(s)	Spectral Resolution				Spatial Resolution		Radiometric Resolution (bits)	Temporal Resolution (days)
					No. of bands, band nos. & spectral range (µm)				Pixel size (m)	Swathe (km)		
30 (10)	EO 1 (USA)	Nov 21, 2000		ALI[xviii]	10	Pan	PAN	0.480-0.680	10	37	12	On demand
						Visible	MS1'	0.433 – 0.453	30			
							MS1	0.450 – 0.510				
							MS2	0.525 – 0.605				
							MS3	0.630 – 0.690				
						NIR	MS4	0.775 – 0.805				
							MS4'	0.845 – 0.890				
							MS5'	1.200 – 1.300				
						MIR	MS5	1.55 – 1.75				
							MS7	2.08 – 2.35				
				Hyperion		220[xix]		0.433-2.35	30	7.7		
31 (11)	EROS A1 (Israel)	Dec 05, 2000			1	Pan	PAN	0.5 – 0.9	1.8	11.5	11	
32 (12)	QuickBird-2 (USA)	Oct 18, 2001		Pan	1	Pan	PAN	0.45 – 0.90	0.6	16.5	11	5
				Multi-spectral	4	Visible	B1	0.45 – 0.52	2.4			
							B2	0.52 – 0.60				
							B3	0.63 – 0.69				
						NIR	B4	0.76 – 0.90				
33 (13)	Proba-1[xx] ESA	Oct 22, 2001		HRC[xxi]		1	PAN		5	14	12	
				CHRIS[xxii]		19 - 62	Hyperspectral	0.415 – 1.050	25 – 50[xxiii]			
34 (14)	AQUA or EOS PM-1 (USA/Japan)	May 04, 2002		MODIS[xxiv]	Same spectral details as on TERRA satellite							

[xviii] ALI – Advance Land Imager
[xix] Each band has 20nm spectral resolution
[xx] PROBA – Project on-board Autonomy
[xxi] HRC – High Resolution Camera
[xxii] CHRIS - Compact High Resolution Imaging Spectrometer
[xxiii] 25m for 19 bands and 50m for 62 bands
[xxiv] MODIS – Moderate Resolution Imaging Spectrometer

Sr. No.	Satellite (Country)	Launched	De-commissioned/ Failed/ Malfunctioned	Sensor(s)	Spectral Resolution				Spatial Resolution		Radiometric Resolution (bits)	Temporal Resolution (days)
					No. of bands, band nos. & spectral range (µm)				Pixel size (m)	Swathe (km)		
35 (15)	SPOT-5 (France)	May 04, 2002		HRS	2	Visible	For-ward	0.490 – 0.690	5 – 10	120	8	5
							Back-ward					
				HRG-1 HRG-2	1	Pan	PAN	0.475 – 0.710	2.5 – 5	60 or 120		
					4	Visible	XS1	0.50 – 0.59	10			
							XS2	0.61 – 0.68				
						NIR	XS3	0.78 – 0.89				
						SWIR	SWIR	1.58 – 1.75	20			
36 (16)	DMC Alsat-1 (Algeria)	Nov 28, 2002		ESIS	3	Visible	B1	0.52 – 0.62	32	600	10	5
							B2	0.63 – 0.69				
						NIR	B3	0.78 – 0.89				
37 (17)	OrbView-3 (USA)	Jun 26, 2003	[xxv]	Pan	1	1	PAN	0.45 – 0.90	1	8	11	5
				Multi-spectral	4	Visible	B1	0.45 – 0.52	4			
							B2	0.52 – 0.60				
							B3	0.625 – 0.695				
						NIR	B4	0.76 – 0.90				
38	DMC BilSat-1 (Turkey)	Sep 27, 2003		PanCam		1	PAN		12	25		
				MSIS		4	B1	0.448 – 0.516	28	5	10	
							B2	0.523 – 0.605				
							B3	0.629 – 0.690				
							B4	0.774 – 0.900				
				COBAN		8	B1	0.375 – 0.425	120	76.8		
							B2	0.410 – 0.490				
							B3	0.460 – 0.540				
							B4	0.510 – 0.590				
							B5	0.560 – 0.640				
							B6	0.610 – 0.690				
							B7	0.660 – 0.740				
							B8	0.850 – 1.000				

[xxv] OrbView-3 has not been able to make usable imagery since Mar 12, 2007

Sr. No.	Satellite (Country)	Launched	De-commissioned/ Failed/ Malfunctioned	Sensor(s)	Spectral Resolution				Spatial Resolution		Radiometric Resolution (bits)	Temporal Resolution (days)
					No. of bands, band nos. & spectral range (µm)				Pixel size (m)	Swathe (km)		
39 (18)	DMC NigeriaSat-1 (Nigeria)	Sep 27, 2003		Same spectral details as DMC AlSat-1								
40 (19)	DMC UK-DMC or BNSCSat-1 (UK)											
41 (20)	ResourceSat-1 or IRS 6P (India)	Oct 17, 2003		LISS-III	4	Visible	B1	0.52 – 0.59	23.5	141	7	
							B2	0.62 – 0.68				
						NIR	B3	0.77 – 0.86				
						SWIR	B4	1.55 – 1.75				
				LISS-IV	3	Visible	B1	0.52 – 0.59	5.8	24	10	
							B2	0.62 – 0.68				
						NIR	B3	0.77 – 0.86				
				AWiFS	4	Visible	B1	0.52 – 0.59	56	744	10	
							B2	0.62 – 0.68				
						NIR	B3	0.77 – 0.86				
						SWIR	B4	1.55 – 1.75				
42 (21)	CBERS-2 (China / Brazil)	Oct 21, 2003		Same spectral details as CBERS-1 satellite								
43 (22)	FormoSat or RocSat2 (Taiwan)	Apr 20, 2004		RSI	5	Pan	PAN	0.490 – 0.900	2	24	8	
						Visible	B1	0.450 – 0.520	8			
							B2	0.520 – 0.600				
							B3	0.630 – 0.690				
						NIR	B4	0.760 – 0.900				
44 (23)	CartoSat-1 or IRS P5 (India)	May 04, 2005		PAN-F	1	Pan	PAN	0.50 – 0.75	2.5	30	10	
				PAN-A	1							
45 (24)	Monitor E1 (Russia)	Aug 26, 2005	[xxvi]		4	Pan	PAN	0.536 – 0.843	8	96		
						Visible	B1	0.528 – 0.585	20	160		
							B2	0.626 – 0.672				
						NIR	B3	0.783 – 0.883				
46 (25)	DMC Beijing1 (China)	Oct 27, 2005		CMT	1	Pan	PAN	0.50 – 0.80	4	24		
				ESIS	3	Visible	B1	0.52 – 0.62	32	600	10	
							B2	0.63 – 0.69				
						NIR	B3	0.78 – 0.89				

[xxvi] Communication failed again on Feb 13, 2007

Sr. No.	Satellite (Country)	Launched	De-commissioned/ Failed/ Malfunctioned	Sensor(s)	Spectral Resolution				Spatial Resolution		Radiometric Resolution (bits)	Temporal Resolution (days)
					No. of bands, band nos. & spectral range (µm)				Pixel size (m)	Swathe (km)		
47 (26)	TopSat (UK)	Oct 27, 2005		RALCam [xxvii]	4	Pan	PAN	0.50 – 0.70	2.8	17		
						Visible	B1	0.40 – 0.50	5.8			
							B2	0.50 – 0.60				
							B3	0.60 – 0.70				
48 (27)	ALOS or Daichi (Japan)	Jan 24, 2006		AVNIR-2	4	Visible	B1	0.42 – 0.50	10	70	8	2 – 45 [xxviii]
							B2	0.52 – 0.60				
							B3	0.61 – 0.69				
						NIR	B4	0.76 – 0.89				
				PRISM [xxix]	3	Visible	Nadir	0.52 – 0.77	2.5	70	8	
							After			35		
							Back					
49 (28)	EROS B1 (Israel)	Apr 25, 2006		PIC-2	1	Pan	PAN	0.50 – 0.90	0.7	14	10	
50 (29)	Resurs DK-1 (Russia)	Jun 15, 2006			4	Pan	PAN	0.58 – 0.80	1	28		
						Visible	B1	0.50 – 0.60	3			
							B2	0.60 – 0.70				
							B3	0.70 – 0.80				
51 (30)	KOMPSAT-2 Arirang-2 (South Korea)	Jul 28, 2006		MSC [xxx]	5	Pan	PAN	0.50 – 0.90	1	15	10	
						Visible	MS1	0.45 – 0.52	4			
							MS2	0.52 – 0.60				
							MS3	0.63 – 0.69				
						NIR	MS4	0.76 – 0.90				
52 (31)	CartoSat-2 or IRS 2A (India)	Jan 10, 2007		PAN	3	Pan	Nadir	0.45 – 0.85	0.8	9.6	10	
							After					
							Back					

[xxvii] RALCam – Rutherford Appleton Laboratory Camera
[xxviii] Revisit time is reduced up to 2 days due to its side viewing capability
[xxix] PRISM - Panchromatic Remote sensing Instrument for Stereo Mapping
[xxx] MSC – Multi-spectral Camera